FE-2028-11
Dist. Category UC-90d

KINETICS AND MECHANISM OF DESULFURIZATION AND DENITROGENATION OF COAL-DERIVED LIQUIDS

Ninth Quarterly Report for Period

June 21, 1977, to September 20, 1977

Prepared by:

Bruce C. Gates, James R. Katzer,
Jon H. Olson, Harold Kwart, and Alvin B. Stiles

Departments of Chemical Engineering and Chemistry
University of Delaware
Newark, Delaware 19711

Date Published

May 1, 1978

Prepared for

Fossil Energy
Department of Energy
Washington, D.C.

Under Contract No. E(49-18)-2028

DISCLAIMER

Available from:

National Technical Information Service (NTIS)
U.S. Department of Commerce
5285 Port Royal Road
Springfield, Virginia 22161

Price: Printed copy: $6.00
Microfiche: $3.00

TABLE OF CONTENTS

LIST OF TABLES

LIST OF FIGURES

LIST OF FIGURES (Continued)

I. ABSTRACT

Flow reactor studies of HDS of dibenzothiophene at about 300°C and 100 atm have shown a new dependence of catalyst activity on H_2S concentration at low values. We infer that the catalyst undergoes structural changes during reaction, sometimes becoming sulfur deficient and relatively inactive. It is evidently necessary to maintain the catalyst in a properly sulfided state during reactor startup and operation by avoiding its contacting too little H_2S.

The relative activities of Ni-Mo/Al_2O_3, Co-Mo/Al_2O_3, and Ni-W/Al_2O_3 catalysts for HDN of acridine have been determined, showing that Ni-Mo/Al_2O_3 is the most active. The results are interpreted in the context of the acridine reaction network, in which both the hydrogenation and hydrogenolysis (cracking) reactions are kinetically important.

II. OBJECTIVES AND SCOPE

Objectives

The major objectives of this research are as follows:

i) To develop high-pressure liquid-phase microreactors for operation in pulse and steady-state modes to allow determination of quantitative reaction kinetics and catalytic activities in experiments with small quantities of reactants and catalyst.

ii) To determine reaction networks, reaction kinetics, and relative reactivities for catalytic hydrodesulfurization of multi-ring aromatic sulfur-containing compounds found in coal-derived liquids.

iii) To determine reaction networks, reaction kinetics, and relative reactivities for catalytic hydrodenitrogenation of multi-ring aromatic nitrogen-containing compounds found in coal-derived liquids.

iv) To obtain quantitative data characterizing the chemical and physical properties of aged hydroprocessing catalysts used in coal liquefaction processes and to establish the mechanisms of deactivation of these hydroprocessing catalysts.

v) To develop reaction engineering models for predicting the behavior of coal-to-oil processing and of catalytic hydroprocessing of coal-derived liquids and to suggest methods for improved operation of hydrodesulfurization and hydrodenitrogenation processes.

vi) In summary, to recommend improvements in processes for the catalytic hydroprocessing of coal-derived liquids.

Scope

A unique high-pressure, liquid-phase microreactor is being developed for pulse (transient) and steady-state modes of operation for kinetics measurements to achieve objectives ii) through iv). The relative reactivities of the important types of multi-ring aromatic compounds containing sulfur and nitrogen are being measured under industrially important conditions (300-450°C and 500-4000 psi). The reaction networks and kinetics of several of the least-reactive multi-ring aromatic sulfur-containing and nitrogen-containing compounds commonly present in coal-derived liquids are being determined. Catalyst deactivation is an important aspect of the commercial scale upgrading of coal-derived liquids. Accordingly, the chemical and physical properties of commercially aged coal-processing catalysts are being determined to provide an understanding of catalyst deactivation; these efforts can lead to improved catalysts or procedures to minimize the problem. To make the results of this and related research most useful to DOE, reaction engineering models of coal-to-oil processing in trickle-bed and slurry-bed catalytic reactors including deactivation will be developed to predict conditions for optimum operation of these processes. Based on the integrated result of all of the above work, recommendations will be made to DOE for improved catalytic hydrodesulfurization and hydrodenitrogenation processes.

III. SUMMARY OF PROGRESS TO DATE

This summary is organized to parallel the task statements of the contract. A milestone chart is provided at the end of this section.

Microreactor Development

Three continuous-flow, liquid-phase, high-pressure microreactors have been built and operated under this contract. The work in this report confirms the success of these microreactors; the data from the batch autoclave runs are effectively identical to data from the flow microreactors. This task has been completed.

Catalytic Hydrodesulfurization

The hydrodesulfurization of dibenzothiophene (DBT) has been examined with a high-pressure microreactor and in batch, stirred-autoclave experiments. The range data show that the reaction network is slightly more complex than the direct reduction of DBT to hydrocarbon products; the network is the following at 300°C and 100 atm:

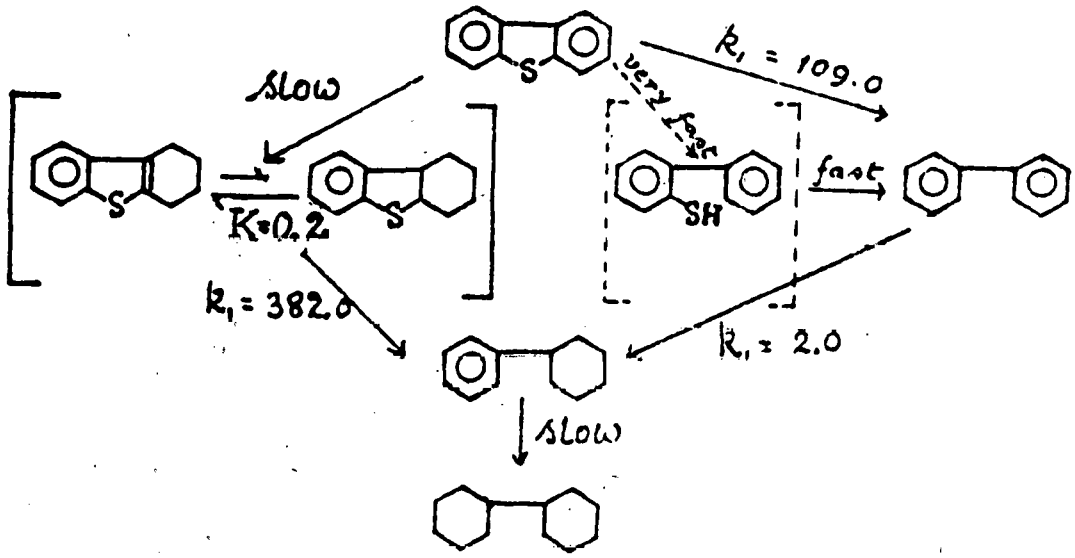

The relative rates of hydrodesulfurization of a variety of the important compounds in coal-derived liquids have been determined. The compounds include methyl-substituted dibenzothiophenes, which evidently are among the least reactive compounds in hydrodesulfurization. The relative rate constants for the various reactants are the following: BT, very large; DBT, 1; 4-MeDBT, 0.16; 4,6-diMeDBT, 0.10; 3,7-diMeDBT, 1.7; and 2,8-DiMeDBT, 2.6. These results are largely explained by steric and inductive effects. Groups located near the S atom restrict its interaction with a surface anion vacancy and lower the reactivity. Inductive effects explain the higher reactivities of the compounds having methyl substituents where they exert no steric influence. The reactivities of the compounds

are influenced by competitive adsorption determined by the previously mentioned steric and inductive effects.

Three different catalysts, namely Co-Mo/γ-Al_2O_3, Ni-Mo/γ-Al_2O_3 and Ni-W/Al_2O_3 have so far been tested for the hydrodesulfurization of dibenzothiophene. The activities of these catalysts per unit mass have been found to decrease in the order: Ni-Mo > Ni-W $\geq$ Co-Mo.

The Co-Mo/Al_2O_3 catalyst appears to undergo structural changes during reaction of DBT, and the sulfur-deficiency which may result and a lack of activity corresponding to it can be prevented by contacting the catalyst with H_2S in sufficient concentrations, which are quite low.

Catalytic Hydrodenitrogenation

The Hydrodenitrogenation of quinoline has been studied to yield a nearly complete identification of the reaction network and partial identification of the rate parameters in this network. The network is as follows:

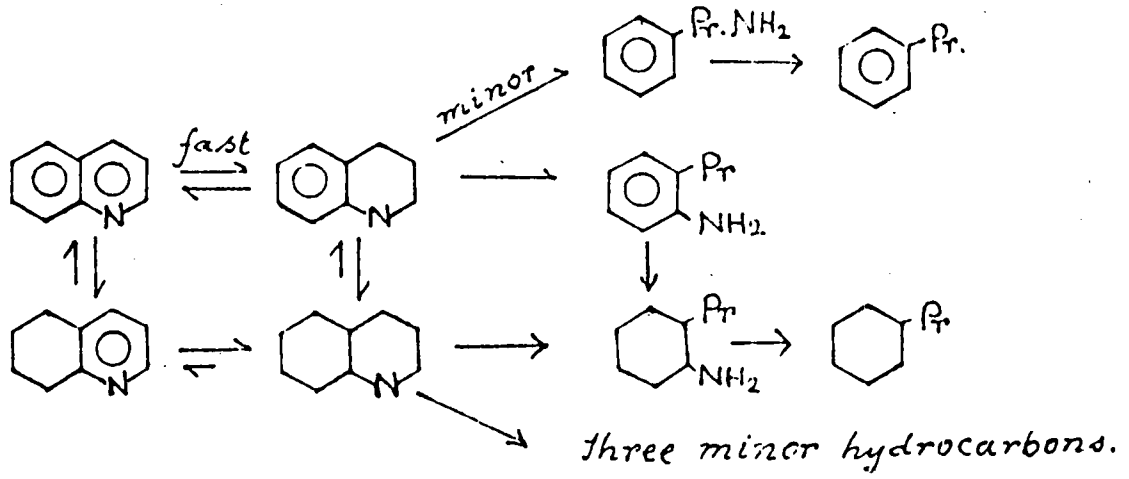

This network shows that usually both the benzene and pyridine rings are saturated before the C-N bond in the (now) piperidine ring is broken. Thus, the HDN of quinoline requires a large consumption of hydrogen before the N atom is removed from the hydrocarbon backbone. The lack of selectivity encountered in hydrodenitrogenation stands in sharp contrast to the high selectivity in hydrodesulfurization.

The total rate of HDN shows a maximum with respect to hydrogen partial pressure. However, the only individual reaction in the network which decreases in rate with increasing hydrogen partial pressure is the conversion of 1,2,3,4-tetrahydroquinoline to ortho-n-propylaniline; this reaction dominates the overall network at high pressure.

Also in hydrodenitrogenation of acridine, a large amount of hydrogenation precedes nitrogen removal, and the carbon-nitrogen bond breaking reactions are relatively slow. In the presence of Co-Mo/γ-Al_2O_3 catalyst, heteroaromatic ring hydrogenation is favored and with a Ni-Mo/γ-Al_2O_3 catalyst, aromatic ring hydrogenation is favored. For both acridine and quinoline, little effect of replacing Co with Ni could be detected in the nitrogen removal reaction, although Ni-Mo/γ-Al_2O_3 is roughly twice as active for hydrogenation as Co-Mo/γ-Al_2O_3.

The hydrodenitrogenation of carbazole has been examined under conditions similar to those used for acridine. Both carbazole disappearance and total nitrogen removal can be represented as first order reactions. Tetrahydrocarbazole was the major intermediate compound present in the dry column extract. Both Cis hexahydrocarbazole and octahydrocarbazole were identified as minor products. Reactivity of carbazole is similar to that of quinoline, and acridine is the least reactive.

Preliminary experiments have been carried out to characterize hydrodenitrogenation of substituted quinolines. The conditions used were similar to those used for quinoline HDN. 2,6-, 2,7- and 2,8-dimethylquinoline were studied and products identified were analogous to those observed in quinoline network. The reactivity of these compounds to HDN is comparable to that of quinoline.

Catalyst Deactivation

A variety of physical techniques have been used to identify the aging processes for catalysts used in synthetic liquid fuel processes. Catalyst samples from three processes have been examined: a proprietary fixed-bed process, Synthoil, and H-Coal^R. The spent fixed-bed catalysts show the formation of an external crust which appears to be formed by columnar grain growth combined with the deposition of coal mineral matter, particularly clays and rutile. This external crust is absent from the H-Coal^R catalyst. The interior of the catalyst is altered by several processes: coking, reactive deposition of mineral matter, passive deposition of mineral matter, and crack enhancement. These four processes are found in catalysts from all three processes. Coking fills the micropore volume of the catalyst. Reactive deposition of mineral matter penetrates about 200 μm from the outer surface into the interior of the catalyst. The concentration profile is approximatoly exponentially decreasing from the exterior surface. Passive cementing occurs within 50 μm of the surface unless the cracks have been enlarged by grain growth; this deposition yields irregular concentration profiles. Finally, grain growth can occur inside the catalyst near the surface and tends to increase these cracks. When the surface cracks become a significant portion of the pore volume, passive deposition can penetrate further into the interior of the catalyst.

The activity of aged catalyst from the H-Coal^R process has been measured in batch experiments with dibenzothiophene and with quinoline. The activity was reduced 20-fold for HDS of dibenzothiophene and five-fold for HDN of quinoline. Burning off of carbonaceous deposits increased the

activity of the aged catalyst only three-fold for dibenzothiophene HDS, which implies that irreversibly deposited inorganic matter was responsible for most of the loss of catalytic activity.

Microreactor Engineering

The use of moments as a tool in interpreting pulse data from microreactors has been extended to fairly complex reaction networks. This work is now complete. The complex data for quinoline and acridine reactions have been reduced to rate parameters by extension of nonlinear regression analysis.

TIME PLAN* AND MILESTONE CHART**

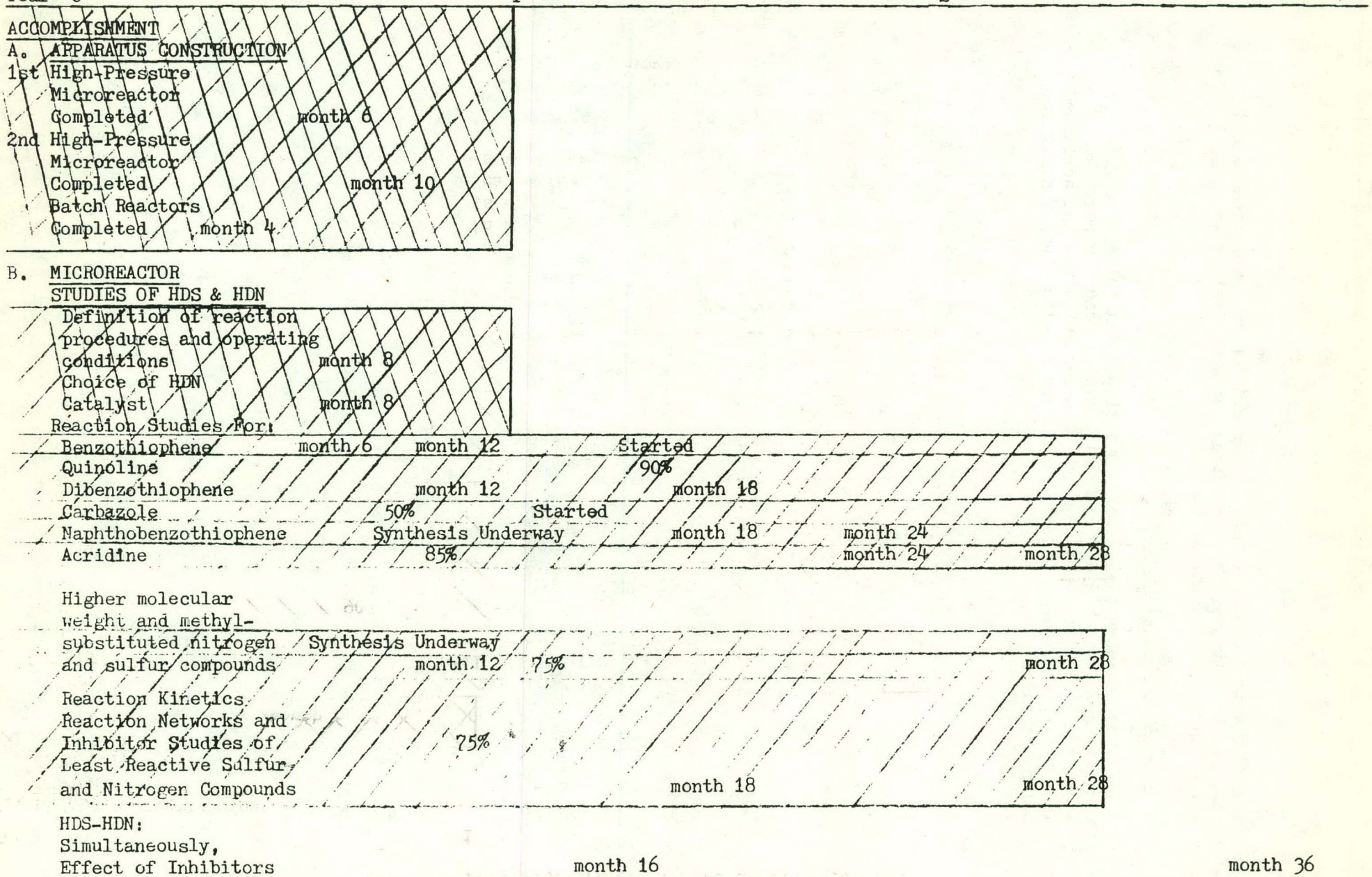

TIME PLAN* AND MILESTONE CHART** (cont'd)

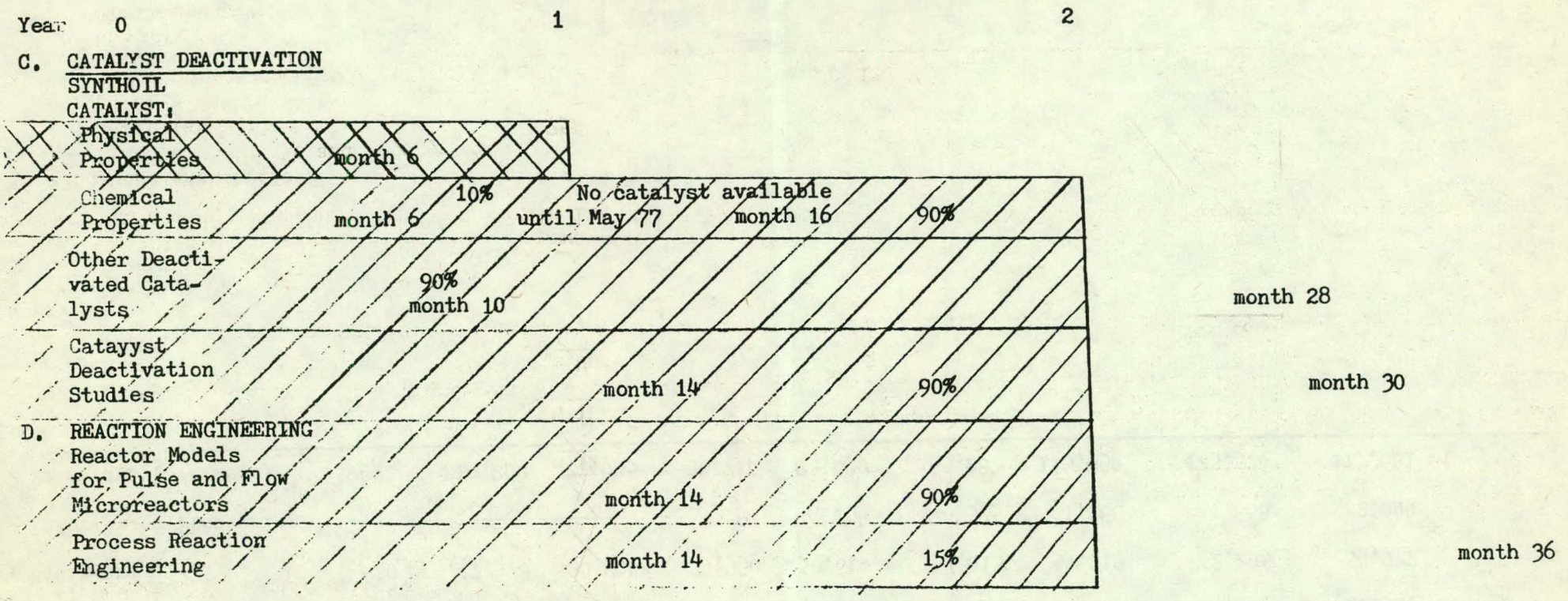

*Time Plan and Milestone Chart as presented in Proposal.

**Hatching indicates that activity indicated is under active investigation; number in hatched region indicates the percentage completed; crosshatching indicates that the task has been completed.

CUMULATIVE EXPENDITURES*

Item	First	Second	Third	Fourth	Fifth	Sixth	Seventh	Eighth	Ninth
Personnel	$5,807	$20,740	$37,396	$53,413	$91,593	$112,666	$132,669	$146,146	$167,884
Travel	28	528	2,152	1,152	1,521	2,458	3,140	3,814	5,119
Supplies & Expense	4,674	10,007	19,582	25,735	37,291	42,341	51,589	56,488	64,778
Occupancy & Maintenance	6,110	9,208	10,108	10,634	13,755	13,920	14,396	14,600	16,325
Equipment	610	17,978	30,704	34,930	50,614	54,013	54,013	52,295	54,977
Information Processing	---	---	---	97	154	375	1,180	1,868	2,044
Transfers (Overhead)	---	10,202	20,035	38,710	75,839	93,287	113,830	123,576	117,681

*Includes encumbrances

IV. DETAILED DESCRIPTION OF TECHNICAL PROGRESS

A. Hydrodesulfurization

The Sulfided Co-Mo/γ-Al_2O_3 Catalyst: Evidence of Structural Changes During Hydrodesulfurization of Dibenzothiophene

Introduction

The catalysts most often used for hydrodesulfurization (HDS) of petroleum and coal-liquid fractions are derived from oxides of Co and Mo supported on γ-Al_2O_3, and their surfaces are sulfided prior to operation. Structures of the oxidic and sulfidic forms of the catalyst are incompletely understood and much debated (1-3), and since the available structural information has been derived from studies of catalysts at conditions far removed from those of commercial operation (about 50-200 atm and 350-320°C), it is not clear how operating variables influence the catalyst structure and activity in practice.

The hydrodesulfurization kinetics data reported here were measured to characterize the catalyst operating at about 100 atm and 300°C; the reactant stream contained dibenzothiophene (DBT) and hydrogen dissolved in n-hexadecane carrier oil. The results provide the first evidence of structural variations in the Co-Mo/γ-Al_2O_3 catalyst brought about by changes in the reaction environment.

Experimental Methods

The catalyst used in all experiments was American Cyanamid HDS 16A having the following properties (prior to sulfiding): surface area, 176 m^2/g; pore volume, 0.50 cm^3/g; Co content, 4.4 wt %; and Mo content, 7.5 wt %. A sample of 10 mg of catalyst powder (80-100 mesh particles, demonstrated

experimentally to be small enough to ensure the lack of intraparticle diffusion resistance) was charged to the reactor, and the catalyst was sulfided at 400°C for 2 hr with a flow of about 40 cm^3/min of 10% H_2S in H_2 at atmospheric pressure. Following the sulfiding, the flow of feed liquid was started. The feed contained 0.12 wt % DBT (Aldrich, 95% purity) in n-hexadecane [Humphrey Chemical Co. (redistilled)], and it was saturated with H_2 at 68 atm and room temperature. Occasionally, the feed was saturated with H_2S at various partial pressures before it was saturated with H_2. Experiments were carried out with a flow reactor described in detail elsewhere (4). The reactor operated at 300°C and 104 atm. Under all reaction conditions, the conversion H_2 was < 5%, so the H_2 concentration could be considered to be virtually constant throughout the reactor.

Liquid product samples were collected periodically (without interrupting the reactant flow) and analyzed by glc (5). DBT and H_2 were converted into biphenyl and H_2S. To a first approximation, these were the only products formed; the detailed reaction network is considered separately (6).

Results

Some conversion data are plotted in Fig. A1. They show that the initial conversion at a relatively high inverse space velocity (proportional to reactant-catalyst contact time) increased about 10% over the first 10-20 hr of operation, following by nearly constant conversion for 150 hr or more. When the lined-out conversion was determined for various space velocities the reaction was found to be pseudo-first-order in DBT (5).

Figure A1 shows the results of variations in the space velocity caused by changes in the feed flow rate. After the first step change in

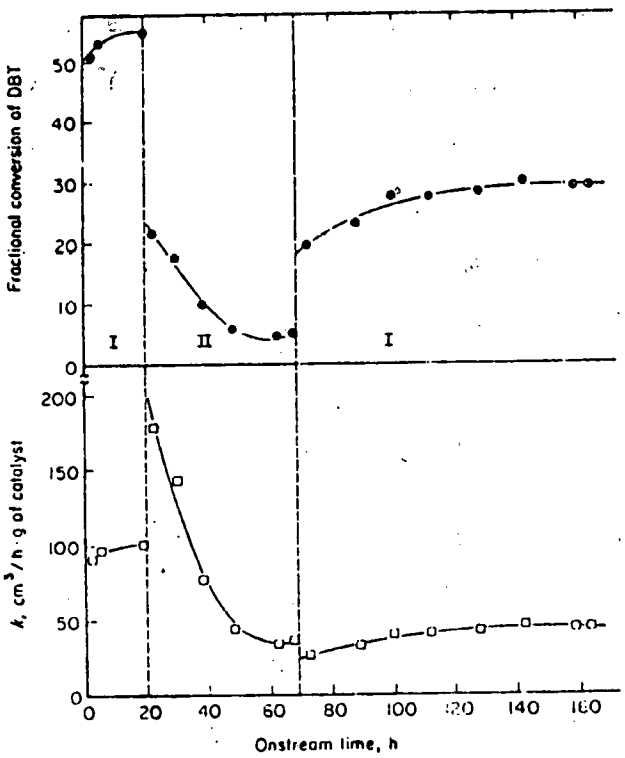

Fig. A1. Conversion and pseudo-first-order rate constants (k) for HDS of DBT. (I) Space velocity = 128 $cm^3/hr \cdot g$ of catalyst. (II) Space velocity = 730 $cm^3/hr \cdot g$ of catalyst. Feed was 0.12 wt % DBT in n-hexadecane which had been saturated with H_2 at 25°C and 68 atm. The catalyst was American Cyanamide HDS 16A. Reaction conditions: 300°C and 104 atm.

feed flow rates, there was a change in conversion characterized by a transient period of some 50 hr before the catalyst achieved another time-invarient activity. After a second change in space velocity at 70 hr onstream time, giving again the original value, there followed a transient period, as expected, but, surprisingly, the catalyst failed to return to its original lined-out activity.

In further experiments, each begun with a fresh catalyst charge, increasing concentrations of H_2S were added to the feed. The data of Fig. A2 show that, at low H_2S concentrations [$(H_2S)/(H_2)$ in the feed liquid = 0.015], the qualitative pattern of changes mentioned above again occurred, but the transients were shorter. The catalyst activity in the presence of added H_2S at each space velocity appeared to be less than that in the absence of added H_2S, corresponding to the well-known inhibition of reaction by H_2S (1,6). When higher feed concentrations of H_2S were used, the transient periods of change in the catalyst activity became shorter; when the $(H_2S)/(H_2)$ ratio in the feed was as great as 0.2, the transients in catalyst activity were almost eliminated.

In summary, these results show that H_2S does more than just inhibit the HDS reaction by adsorbing on catalytic sites in competition with DBT. We infer that, when the space velocity was increased, reducing the concentration of H_2S produced in the reaction (Figs. A1 and A2), structural changes took place, reducing the number of catalytic sites. The presumed solid-state reactions were slow, in contrast to the adsorption of H_2S that caused the inhibition of reaction. The presumed loss of

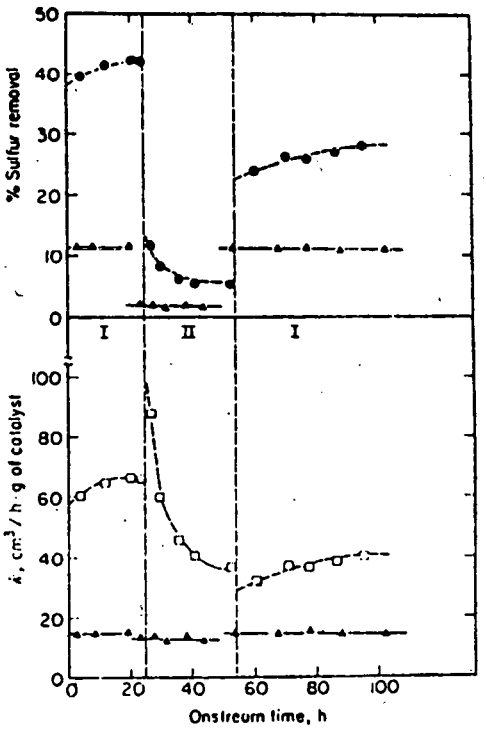

Fig. A2. Conversion and pseudo-first-order rate constants ($\underline{k}$) for HDS of DBT. (I) Space velocity = 124 $cm^3/hr \cdot g$ of catalyst. (II) Space velocity = 705 $cm^3/hr \cdot g$ of catalyst. Concentration ratios $[(H_2S):(H_2)]$ = 0.2 (-Δ-) and 0.015 (-O-). The feed, catalyst, and reaction conditions were the same as those described in the legend to Fig.A1, except for the added H_2S.

of catalytic sites was only partially reversed when the concentration of H_2S was present in the feed in amounts sufficient for the H_2S concentration to remain nearly constant throughout the reactor, the catalyst activity did not change with space velocity; the data then indicate only the simple competitive inhibition of reaction by H_2S.

The foregoing results suggest that there is an optimum concentration of H_2S [or perhaps a $(H_2S):(H_2)$ ratio] corresponding to a catalytic structure which has a maximum HDS activity. Experiments were carried out to test this suggestion. In one series, catalysts were brought on stream with initially low space velocities, producing initially high activities; the experiments were done with various feed H_2S concentrations. The pseudo-first-order rate constants are represented by curve B in Fig. A3; they indicate that in these experiments the H_2S was simply a reaction inhibitor.

In other experiments, each new catalyst charge was brought on stream at a high space velocity and, correspondingly, with a relatively low conversion and a low H_2S concentration; H_2S concentration in the feed was varied systematically. The rate constants scatter around curve A in Fig. A3. Conversions determined with catalysts initially brought on stream at low space velocity and subsequently allowed to attain steady state at high space velocity also gave points scattering around curve A. The results show that increasing H_2S concentrations correspond to increasing activities of catalysts which have attained steady activity at low H_2S concentrations. There was an apparent irreversibility. These catalysts did not attain the activities associated with curve B, even when the $(H_2S):(H_2)$ ratio was increased into the range of overlap of curves A and B.

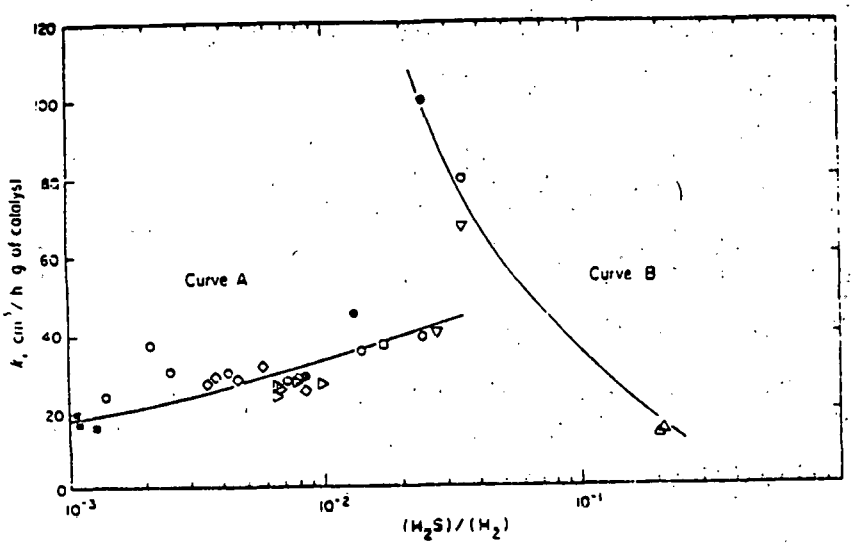

Fig. A3. Effects of H_2S on activity of the catalyst for HDS of DBT under the reaction conditions given in the legend to Fig. A1. The points on curve A represent conversion measured at various space velocities and with various feed $[(H_2S):(H_2)]$ ratios for catalysts which had previously attained time-invariant activities at high space velocities (700-750 $cm^3/hr \cdot g$ of catalyst). These results imply that the catalyst which attained time-invariant activities at high space velocities were sulfur deficient and relatively inactive, becoming more active on addition of H_2S, as discussed in the text. The points on curve B represent conversion measured at various feed $[(H_2S):(H_2)]$ ratios for catalysts which had previously attained time-invariant activities at low space velocities (90-100 $cm^3/hr \cdot g$ of catalyst). These results indicate competitive inhibition of reaction by H_2S. See text for details.

The important conclusion is that the catalyst achieves a lined-out activity which is dependent on the reactor startup procedure (and probably on the presulfiding procedure as well). This conclusion may be important to the technology of HDS, and we suggest that the industrial art may include the application of presulfiding and reactor startup procedures which maximize the catalyst activity; the optimum startup would ensure that some H_2S contacted the catalyst initially.

Discussion

The observed changes in catalytic activity and, by inference, catalyst structure, are suggestive of Farragher's (7) observations of the activity of Ni-W/γ-Al_2O_3 catalyst for benzene hydrogenation. Farragher presented evidence of hysteresis effects similar to those reported here, but caused by temperature variations; he explained the results in terms of solid-state reactions influencing catalyst structure and activity. The suggested reactions were the following:

$$3V_s + Ni_3S_2 + 2H_2 \rightleftarrows 3Ni_s + 2H_2S \qquad (1)$$

$$2W^{4+} + Ni_s \rightleftarrows 2W^{3+} + Ni_s \qquad (2)$$

The former reaction involves conversion of Ni from bulk Ni_3S_2 on the catalyst; it becomes intercalated in interstitial octahedral holes at the surface of WS_2 crystallites on the catalyst surface. The latter reaction is believed to produce W^{3+} ions at the surface, which Voorhoeve et al. (8,9) have characterized by esr and identified as the catalytic sites for benzene hydrogenation. Farragher showed that both the rate constant for benzene

hydrogenation and the esr signal indicative of W^{3+} were dependent on the P_{H_2S}/P_{H_2} ratio in a way that is consistent with the catalyst stoichiometry suggested in Eqs. (1) and (2).

There is much evidence (1,11) [but not a concensus (2,3)] supporting the view that the Co-Mo/γ-Al_2O_3 catalyst is similar to the Ni-W/γ-Al_2O_3 catalyst, consisting of MoS_2 and Co_9S_8 on the Al_2O_3 surface, and esr evidence supports the idea that the catalytic sites are Mo^{3+} ions intercalated at the edges of the MoS_2 crystallites (1,7,12).

Following Farragher, and assuming the validity of the edge intercalation model for the Co-Mo catalyst, we suggest the following speculative interpretation of the structural changes in the catalyst brought about by changes in the reaction environment. The fully active catalyst is supposed to consist of MoS_2 crystallites intercalated with Co^{2+} ions, and H_2S can bond to the surface at anion vacancies in competition with DBT, causing inhibition of the HDS reaction. When only little H_2S is present, however, intercalated MoS_2 may be converted into a sulfur-deficient layer structure which may lack catalytic activity. We speculate that $CoMo_2S_4$ may be the sulfur-deficient structure, since it is known to lack HDS activity and to have the layer structure shown in Fig. A4 (10). Here both Co^{2+} and Mo^{3+} ions are octahedrally surrounded by S^{2-} ions, whereas in MoS_2 the surrounding is trigonal prismatic.

It is important that $CoMo_2S_4$ meets the criterion of having a lower sulfur content than the presumed catalyst, Co-intercalated MoS_2; to explain the observed intermediate activities, we suggest that the catalyst may

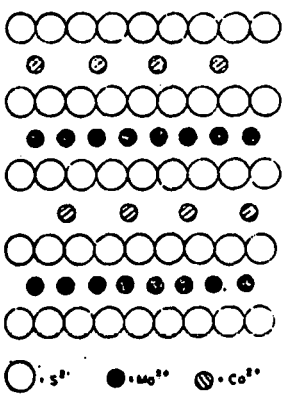

Fig. A4. Representation of the layer structure of $CoMo_2S_4$. The actual structure is distorted, as shown by van den Berg (10).

consist of a range of intermediate structures which could be interconverted by local redistributions of Co and Mo ions accompanied by changes in the Mo-S surrounding.

An explicit suggestion is the epitaxial structure shown in Fig. A5. This structure accounts for the observed promotion by Co at higher Co/Mo ratios than can be accounted for by the edge intercalation model (11). It might be expected to undergo changes analogous to those postulated by Farragher for the Ni-W catalyst:

$$9V_2 + Co_9S_8 + 16H_2 \rightleftharpoons 9Co_s + 8H_2S \qquad (3)$$

$$2Mo^{4+} + Co_s \rightleftharpoons 2Mo^{3+} + Co_s^{2+} \qquad (4)$$

This model is not consistent with the experimental evidence; it is rough and speculative and in need of experimental evaluation.

Notation

- k pseudo-first-order rate constant, $cm^3/h \cdot g$ of catalyst
- p partial pressure
- V_s interstitial octahedral hole in a layer structure like MoS_2

References for Part A

1. de Beer, V. H. J., and Schuit, G. C. A., Ann. New York Acad. Sci. 272, 61 (1976).
2. Delmon, B., Preprints ACS Div. Petrol. Chem. 22 (2), 503 (1977).
3. Massoth, F. E., J. Catal. 50, 190 (1977).
4. Eliezer, K. F., Bhinde, M., Houalla, M., Broderick, D., Gates, B. C., Katzer, J. R., and Olson, J. H., Ind. Eng. Chem. Fundam. 16, 380 (1977).

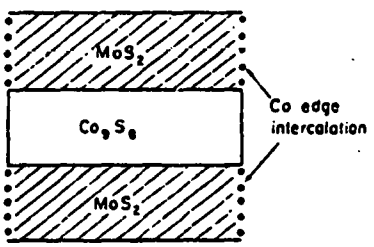

Fig. A5. Model of the sulfided Co-Mo/γ-Al_2O_3 catalyst, representing layers of Co_9S_8 and MoS_2 intercalated with Co^{2+} at the crystal edges.

5. Houalla, M., Broderick, D., de Beer, V. H. J., Gates, B. C., and Kwart, H., Preprints ACS Div. Petrol. Chem. 22, 941 (1977).

6. Houalla, M., Nag, N. K., Sapre, A., Broderick, D. H., and Gates, B. C., to be published.

7. Farragher, A. L., paper presented at ACS meeting, New Orleans, March, 1977.

8. Voorhoeve, R. J. H., and Stuiver, J. C. M., J. Catal. 23, 228, 243 (1971).

9. Voorhoeve, R. J. H., J. Catal. 23, 236 (1971).

10. van den Berg, J. M., Inorg. Chim. Acta. 2, 216 (1968).

11. Furimsky, E., and Amberg, C. H., Can. J. Chem. 53, 2542 (1975).

12. Konigsberger, D., comments accompanying paper B23, Sixth International Congress on Catalysis, London, 1976.

B. Hydrodenitrogenation

Introduction

There has recently been increased interest in the hydrodenitrogenation of nitrogen-containing aromatic compounds typical of those found in petroleum, coal-derived liquids and shale oils. Because of the high nitrogen contents of coal-derived liquids and shale oil, hydrodenitrogenation will become increasingly important in the future. Mars and coworkers, (Sonnemans, et al., 1974; Sonnemans and Mars, 1973; Sonnemans, et al., 1973a; and Sonnemans, et al., 1973b), and McIlvried (1971) have clarified the reaction network and kinetics associated with the hydrodenitrogenation of pyridine. Their work was done on unsulfided Co-Mo/Al_2O_3 catalyst. Although several authors (Aboul-Gheit and Abdou, 1973; Aboul-Gheit, 1975; Doelman and Vlugter, 1963; and Flinn et al., 1963) have studied the hydrodenitrogenation of quinoline, neither the reaction network nor the reaction kinetics have been adequately defined for this system. We have

recently established the reaction network and reaction kinetics of hydrodenitrogenation of quinoline (Shih et al., 1977; Shih et al., 1977a) and of acridine (Zawadzki et al.) over sulfided hydroprocessing catalyst under high-pressure liquid-phase conditions.

Both the prior literature (Sonnemans et al., 1974; Sonnemans and Mars, 1973; Sonnemans et al., 1973a; Sonnemans et al., 1973b; McIlvried, 1971; Aboul-Gheit and Abdou, 1973; Aboul-Gheit, 1975; Doelman and Vlugter, 1963; Flinn et al., 1963) and our work (Shih et al., 1977; Shih et al., 1977a; Zawadzki et al.) shows that hydrodenitrogenation of nitrogen-containing compounds occurs via a complex reaction network involving hydrogenation of the aromatic rings followed by carbon-nitrogen bond breaking. This is in contrast to hydrodesulfurization, in which sulfur removal occurs directly without hydrogenation of the associated aromatic rings (Houalla et al., 1977). It is therefore important to understand how catalyst composition affects the relative rates of hydrogenation of bond breaking in the complex nitrogen-removal reaction network. This bifunctional nature of the reaction network requires an appropriate balance between the catalyst hydrogenation and catalyst bond-breaking functions to provide the most active catalyst. A quantitative definition of the relative kinetic role of the two catalyst functions in hydrodenitrogenation is not available.

The literature contains several catalyst comparisons for hydrodenitrogenation. Sonnemans, et al. (Sonnemans et al., 1974; Sonnemans and Mars, 1973; Sonnemans et al., 1973a; Sonnemans et al., 1973b) studied the gas-phase hydrodenitrogenation of pyridine, piperidine and n-pentylamine over $MoO_3/\gamma\text{-}Al_2O_3$, $CoO\text{-}MoO_3/\gamma\text{-}Al_2O_3$ and Al_2O_3. They found little difference

in activity and selectivity for $MoO_3/\gamma\text{-}Al_2O_3$ and $CoO\text{-}MoO_3/\gamma\text{-}Al_2O_3$. On the other hand, piperidine showed a 20-fold higher rate of nitrogen removal over $Co\text{-}MoO_3/\gamma\text{-}Al_2O_3$ and Co or Mo oxides as compared to $\gamma\text{-}Al_2O_3$. They concluded that MoO is the active component for hydrogenation, cracking and disproportionation reactions. Satterfield and Coccetto (1975) conclude that $Ni\text{-}Mo/\gamma\text{-}Al_2O_3$ has greater hydrogenation and dehydrogenation activity, whereas a $Co\text{-}Mo/\gamma\text{-}Al_2O_3$ has greater hydrogenolysis activity in the gas-phase hydrodenitrogenation of pyridine. Ahuja et al. (1970) found that the activity for hydrogenating aromatic systems fell in the order: NiW > Ni-Mo > Co-Mo > Co-W for catalysts in the unsulfided form supported as $\gamma\text{-}Al_2O_3$. For hydrogenation of isolated double bands the order was: Ni-W > Co-W > Co-Mo > Ni-Mo. Cir et al. (1972) found that $Ni\text{-}Mo/\gamma\text{-}Al_2O_3$ was more active for hydrodenitrogenation of distilled residues than $Co\text{-}Mo/\gamma\text{-}Al_2O_3$, but both catalysts gave essentially the same degree of hydrodesulfurization. Silver et al. (1972, 1974) found that $Ni\text{-}W/\gamma\text{-}Al_2O_3$ was more selective than $Co\text{-}Mo/\gamma\text{-}Al_2O_3$ in hydrodenitrogenation of quinoline-type compounds, that $Ni\text{-}W/\gamma\text{-}Al_2O_3$ was less active in hydrodenitrogenation of indole type compounds than Co-Mo, that it hydrodenitrogenated quinoline more rapidly and that the behavior of Ni-W was independent of whether it was on $\gamma\text{-}Al_2O_3$ or $SiO_2\text{-}Al_2O_3$. Rollmann (1976) found that $Ni\text{-}Mo/\gamma\text{-}Al_2O_3$ was more active than $Co\text{-}Mo/\gamma\text{-}Al_2O_3$ in hydrodenitrogenation but that the activity of the two catalysts became increasingly similar as the catalysts aged. Goudriaan (1974) found that the sulfided form of the catalyst was three to four times more active for the hydrogenation and hydrogenolysis reactions of pyridine, than the oxidic form. He concluded that the addition of H_2S to the reaction system caused sulfur vacancies to be filled, thus increasing the acidity of the surface and reducing the self-poisoning effect of bases.

Generally Ni-Mo/γ-Al_2O_3 or Ni-W/γ-Al_2O_3 have been reported to be more active for hydrodenitrogenation than Co-Mo/γ-Al_2O_3, the catalyst of choice for hydrodesulfurization, and the enhanced behavior is often assured to be due to higher hydrogenation activity (Flinn et al., 1963; Rollmann, 1977; Yarrington, 1969). This is not confirmed by quantitative experimental data, particularly under typical hydroprocessing conditions with multi-ring nitrogen-containing compounds.

In this work we have evaluated the relative behavior of commercial hydroprocessing catalysts of differing metal composition and support under high-pressure liquid-phase conditions. The catalysts were examined in the oxidic form, sulfided, and sulfided with H_2S in the system. First-order rate constants for all hydrogenation and bond breaking steps in the reaction networks were determined as a function of catalyst type and catalyst pretreatment. Our objectives were to determine how the catalyst type and pretreatment affected the rate of each individual reaction in the hydrodenitrogenation reaction network and thus to elucidate the fundamental differences in the catalysts.

Experimental

The experiments were carried out in a one-liter stirred autoclave (Autoclave Engineer) which was operated in batch mode. The system was designed to withstand 410 atm and was housed behind a barricade. A special reactant-oil-catalyst injection system was attached to the autoclave to inject catalyst and reactant (nitrogen-containing compound) in carrier oil into the autoclave reactor after it had been stabilized at the operating temperature and pressure. Consequently, the problems of reaction and

catalyst deactivation during the long heat-up time frequently encountered in autoclave studies were eliminated, and zero time was precisely defined. The reactor temperature was controlled to ±1°C. A glass liner was used to eliminate wall activity. A porous stainless steel filter (0.5μ pore size) was attached to the end of the hydrogen inlet inside the autoclave to disperse dihydrogen as fine bubbles. A porous filter was also attached to the end of liquid sampling line to filter out catalyst particles. A schematic of the reactor setup is given elsewhere (Shih et al., 1977).

For a typical run the autoclave was brought to reaction temperature and pressure while periodically purging the system with dihydrogen. When the autoclave was at operating conditions, the oil-catalyst-reactant mixture was injected into the autoclave. There was an initial temperature drop that lasted at most 10 min. Liquid samples were withdrawn periodically and were analyzed by gas chromatography.

Unless stated otherwise, the experimental conditions were as stated in Table I.

Experimental Materials

Quinoline, acridine, and 1,2,3,4 tetrahydroquinoline (Aldrich Chemical Co.) were > 99% purity and were used as received. γ-phenylpropyl amine was obtained from ICN Pharmaceuticals, Inc. (Plainview, NY). C.P. grade hydrogen (Matheson) was purified by passing through a DEOXO column (Engelhard Minerals & Chemicals Corp.) and a molecular sieve column to remove trace amounts of oxygen and water respectively. Perhydroacridine was prepared by hydrogenation of acridine. The white oil (Parol 70, Pereco Division of Penzoil Co.) was a prehydrotreated, highly paraffinic

TABLE I

STANDARD OPERATING CONDITIONS

One-liter stirred autoclave, stirring speed 1700 rpm

	Quinoline	Acridine
Temperature, °C	342 ±1	367 ±1
Total pressure, atm	34[a]	136
Catalyst	0.5 wt % in carrier oil, 150-200 mesh	0.5 wt % in carrier oil, 150-200 mesh
Catalyst presulfiding[b]	2 hr at 325°C in 160 cm^3/min flow of 10% H_2S/H_2	2 hr at 425°C in 160 cm^3/min flow of 10% H_2S/H_2
Reactant concentration, wt %	1.0	0.5
Autoclave stirring speed, rpm	1700	1700
Carrier oil, cc	500	500

[a] At 342°C the white oil vapor pressure is about 6.3 atm.

[b] Presulfiding procedure resulted in the catalyst contacting a ten-fold stoichiometric excess of sulfur, where noted 0.05 wt % CS_2 was added to the carrier oil to provide H_2S which kept the catalyst surface in a sulfided state.

oil which was free of sulfur- and nitrogen-containing compounds and aromatics. Its boiling range was 315 to 455°C, and it contained mainly C_{18} to C_{36} hydrocarbons.

The properties of the catalysts studied are given in Table II.

Analytical Techniques

The concentration of the nitrogen-containing reaction products was determined by gas chromatograph (Perkin Elmer Model 3920B) equipped with a nitrogen-phosphorous specific detector, consisting of a rubidium silicate bead placed above the jet of a conventional FID detector. The nitrogen-specific detector eliminates interference by hydrocarbons. For quinoline product analysis a 10' X 1/8" Chromasorb 103 glass column, and 235°C oven temperature were used. An appropriate concentration standard was injected initially and after each fire samples to saturate active sites on the column. For acridine product analysis a 50 m OV101 SCOT glass column and oven temperature of 220°C was used.

A concentration vs. peak area calibration curve was constructed for acridine and was verified before, during and after the analysis of each run. In all cases, the samples were analyzed in a random manner. Repeated injections of the same sample showed a ±10% variation in the concentration of nitrogen compounds.

Results

The reaction network for quinoline hydrodenitrogenation with specific rate constants identified as established by Shih et al. (1977, 1977a) is:

TABLE II

CATALYST PROPERTIES DATA

Catalyst	Ni-Mo/γ-Al_2O_3 (HDS-9A)	Co-Mo/γ-Al_2O_3 (HDS-16A)	Ni-W/γ-Al_2O_3 (NT-550)
Supplier	American Cyanamid	American Cyanamid	Nalco
Composition, wt %			
NiO	3.0-4.0	---	5.1
CoO	---	5.7	---
MoO_3	17.5-18.5	12.2	---
WO_3	---	---	22.0
Na_2O	0.04	0.03	---
Fe	0.05	0.04	---
Surface area, m^2/g	149	176	250
Pore volume, cc/g	0.46	0.425	0.5

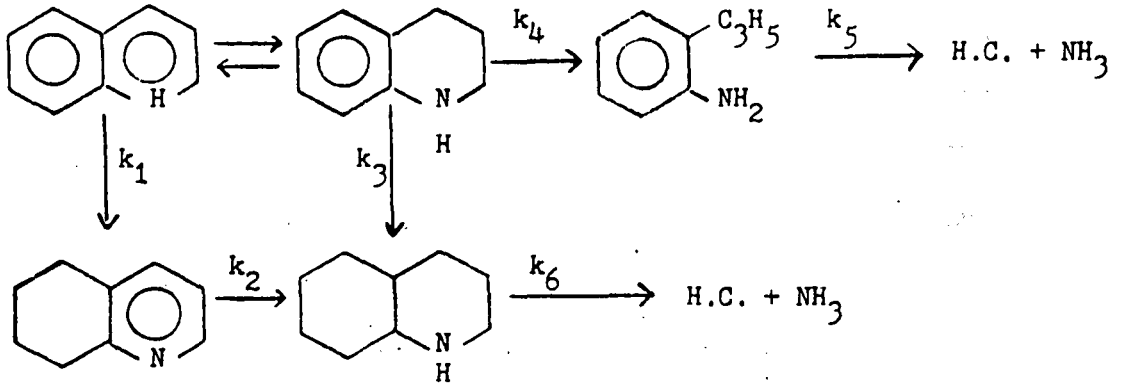

The quinoline reaction network involves a very rapid hydrogenation of the heteroaromatic ring giving thermodynamic equilibrium between quinoline and 1,2,3,4-tetrahydroquinoline. The other ring hydrogenation steps are kinetically much slower. Conversion of o-propylaniline appears to involve hydrogenation of the benzene ring followed by carbon-nitrogen bond rupture (Shih et al., 1977, 1977a). Conversion of 1,2,3,4-tetrahydroquinoline to o-propylaniline and of decahydroquinoline to hydrocarbon and NH_3 clearly involve carbon-nitrogen bond rupture.

The system showed first-order kinetic behavior with respect to the removal of quinoline, acridine and total nitrogen content. Therefore in modeling each reaction in the entire reaction network pseudo first-order kinetics was used. The pseudo first-order rate constants were defined by

$$\frac{M_o}{M_c}\frac{d\,C_i}{dt} = -K_{i,j}\,C_i$$

where

M_o = mass of oil, g
M_c = mass of catalyst, g
C_i = concentration of species i, gmoles i/g oil
t = time, min
$K_{i,j}$ = pseudo first order rate constant for compound i in the jth reaction, (g oil)(g cat-min)$^{-1}$ ≡ min^{-1}

The behavior of different catalysts in quinoline hydrodenitrogenation is given in Table III. Ni-Mo/Al_2O_3 is a slightly better catalyst for the removal of nitrogen from quinoline than Co-Mo/Al_2O_3 or Ni-W/Al_2O_3 as shown by the pseudo first-order rate constants for total nitrogen removal. The Ni-containing catalysts appear to be more active for hydrogenating the benzenoid ring (k_1 and k_3) whereas the Mo-containing catalysts appear to be more active in hydrogenating the heteroaromatic ring (k_2). The pseudo first-order rate constants for the cracking steps (k_4 and k_6) are more dependent on the source of the alumina (catalyst) than on the metals present as demonstrated better by other studies not reported here.

Presulfiding has a marked effect on the total nitrogen removal rate (Table IV); the rate constant for total nitrogen removal almost doubles. However there seems to be little or no gain in going from the oxidic form to the sulfided form of the catalyst in reactions that involve carbon-nitrogen bond breaking. The rates for these reactions remain basically the same, as can be seen upon comparing k_5 and k_6 for the oxidic and sulfided catalyst in Table IV. Presulfiding has a marked influence on the rate of hydrogenation of the benzenoid and heteroaromatic ring (k_1, k_2 and k_3). However, there seems to be a preference for hydrogenation of the benzenoid ring over the heteroaromatic ring in quinoline; there is a 4-fold increase in the value of k_1 and k_3 as compared to only a 1.5-fold increase in k_2. The reaction path involving o-propylaniline is of negligible importance for the oxidic form.

The effect of adding CS_2 (H_2S) on the reaction system is shown in Table V. H_2S increases the rate of total nitrogen removal. The presence of

TABLE III

HYDRODENITROGENATION OF QUINOLINE OVER DIFFERENT CATALYSTS

Rate constant, min^{-1}	Ni-Mo/Al_2O_3 (Cyanamid HDS-9A)	Co-Mo/Al_2O_3 (Cyanamid HDS-16A)	Ni-W/Al_2O_3 (Nalco NT-550)
k_1	3.10	1.49	2.17
k_2	1.11	1.51	0.52
k_3	0.63	0.26	0.33
k_4	0.077	0.067	0.073
k_5	0.61	1.51	0.36
k_6	2.54	3.56	1.11
$k_{Total\ N\text{-}removal}$	0.30	0.20	0.19

Operating conditions: Catalysts were presulfided, no CS_2 added to the system, T = 342°C, P = 34 atm.

TABLE IV

EFFECT OF PRESULFIDING ON THE HYDRODENITROGENATION OF QUINOLINE

	Ni-Mo/Al_2O_3 (Cyanamid HDS-9A)		
Rate constant, min^{-1}	oxidic	presulfided	
k_1	0.72	3.10	(4.3X)
k_2	0.75	1.11	(1.5X)
k_3	0.18	0.63	(3.5X)
k_4	0.0023[a]	0.077	
k_5	0.75	0.61	
k_6	2.2	2.54	
$k_{Total\ N\text{-}removal}$	0.17	0.3	

Operating conditions: catalyst presulfided at 325°C for 2 hr in 10% H_2S/H_2, no CS_2 added, T = 342°C, P = 34 atm.

[a]This value was so small for the oxidic form that its value is uncertain.

H_2S enhances the carbon nitrogen bond breaking rates (i.e., k_6 and particularly k_4). However, k_5 is negatively affected since the transformation of o-propylaniline to a hydrocarbon and ammonia involves first a hydrogenation step (Shih et al., 1977; Shih et al., 1977a); k_5 is a compound pseudo first-order rate constant. Little advantage of having H_2S present in the hydrogenation rates (k_1, k_2 and k_3). For the Co-Mo/Al_2O_3 catalyst there is no enhancement of the hydrogenation of the heteroaromatic ring; but the benzenoid ring hydrogenation capacity is slightly enhanced. For the Ni-Mo/γ-Al_2O_3 and Ni-W/γ-Al_2O_3 the converse is true; they experience a decrease in their benzenoid ring hydrogenation activity and an increase in their heteroaromatic ring hydrogenation activity with gas-phase H_2S.

The difference between Co-Mo/γ-Al_2O_3 and Ni-Mo/γ-Al_2O_3 increase with the severity of the operating conditions as shown in Table VI. Under the more severe operating conditions Ni-Mo/γ-Al_2O_3 is superior by a factor of about 2 for total nitrogen removal rate. The hydrogenation rates (k_1, k_2, k_3, and k_5) are all significantly higher over the Ni-Mo/γ-Al_2O_3 than for the Co-Mo/γ-Al_2O_3. The behavior for nitrogen-carbon bond rupture is consistent with the relative behavior observed for the less severe conditions.

For acridine the hydrodenitrogenation reaction involves the following reaction network (Zawadzki et al., 1977):

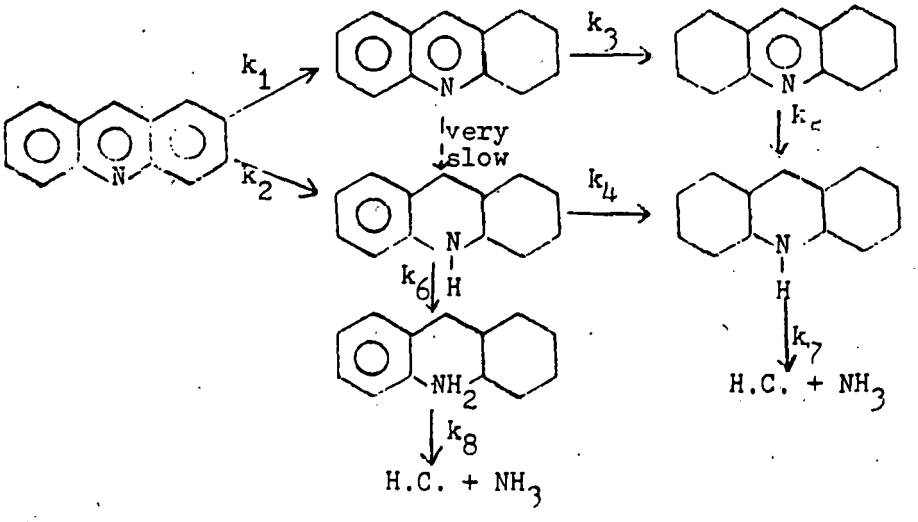

TABLE V

EFFECT OF H_2S ON THE HYDRODENITROGENATION OF QUINOLINE

Rate constant, min^{-1}	Ni-Mo/Al_2O_3 (Cyanamid HDS-9A)		Co-Mo/Al_2O_3 (Cyanamid HDS-16A)		Ni-W/Al_2O_3 (Nalco NT-550)	
	A	B	A	B	A	B
k_1	3.10	3.09	1.49	1.51	2.17	1.71
k_2	1.11	1.57	1.51	1.51	0.52	1.24
k_3	0.63	0.32	0.26	0.24	0.33	0.21
k_4	0.073	0.13	0.067	0.18	0.073	0.15
k_5	0.61	0.13	1.51	0.78	0.36	0.38
k_6	2.54	3.89	3.56	3.64	1.11	2.94
$k_{total\ N_2\ removal}$	0.30	0.57	0.20	0.41	0.19	0.60

Operating conditions: All catalysts were presulfided at 325°C in 10% H_2S/H_2 for 2 hrs, T = 342°C, P = 34 atm.
A: without CS_2; B: with 0.05 wt % of CS_2 in white oil to give gas phase H_2S.

TABLE VI

CATALYTIC HYDRODENITROGENATION OF QUINOLINE AT MORE SEVERE CONDITIONS

Rate constant, min^{-1}	$Ni-Mo/Al_2O_3$ (Cyanamid HDS-9A)		$Co-Mo/Al_2O_3$ (Cyanamid HDS-16A)	
	mild*	severe**	mild*	severe**
k_1	3.09	4.95	1.51	0.69
k_2	1.57	10.55	1.51	2.95
k_3	0.32	4.67	0.24	2.28
k_4	0.13	0.50	0.18	0.51
k_5	0.13	3.40	0.78	1.91
k_6	3.89	10.58	3.64	3.45
$k_{\text{total N-removal}}$	0.57	2.42	0.41	1.22

All catalysts presulfided at 325°C in 10% H_2S/H_2 for 2 hrs, 0.05 wt % CS_2 was added to all runs.

*mild operating conditions: temp., 342°C; total pressure, 34 atm.

**severe operating conditions: temp, 367°C; total pressure, 136 atm.

The reaction network again involves hydrogenation reactions followed by carbon-nitrogen bond breaking reactions with saturation of the aromatic ring structure required before carbon-nitrogen bond breaking can occur. Acridine is hydrogenated to tetrahydroacridine and octahydroacridine with further hydrogenation steps to produce the completely hydrogenated perhydroacridine molecule which then can undergo carbon-nitrogen bond breaking to produce ammonia and a hydrocarbon, octahydroacridine, as in the case of 1,2,3,4 tetrahydroquinoline, can also undergo a bond breaking process to give o-methylcydohexyl aniline which then can undergo hydrogenation and carbon-nitrogen bond rupture to give a hydrocarbon and ammonia. The effect of different catalysts on the hydrodenitrogenation of acridine is shown in Table VII. Hydrogenation rates (k_1, k_2, k_3, k_4, and k_5) are typically more rapid over the Ni-Mo/γ-Al_2O_3 and Ni-W/γ-Al_2O_3 catalysts than over the Co-Mo/γ-Al_2O_3; the Ni-Mo/γ-Al_2O_3 catalyst has a slight advantage over Ni-W/γ-Al_2O_3. The Ni-Mo/γ-Al_2O_3 catalyst shows distinctly higher activity for the carbon-nigrogen bond rupture steps and thus is overall the superior of the catalysts used in these studies.

Discussion

Quinoline hydrodenitrogenation

The relative behavior of the different catalysts can best be demonstrated by considering the ratio of the rate constants for each of the steps in the reaction network. The comparison for

[Ni-Mo/γ-Al_2O_3] / [Co-Mo/γ-Al_2O_3]

and for [Ni-W/γ-Al_2O_3] / [Co-Mo/γ-Al_2O_3]

in quinoline hydrodenitrogenation without added CS_2 is shown in Figure B1. Figure B2 shows the same comparison for quinoline hydrodenitrogenation with

TABLE VII

EFFECT OF CATALYST TYPE ON THE HYDRODENITROGENATION OF ACRIDINE

Rate constant, min^{-1}	Ni-Mo/Al_2O_3 (Cyanamid HDS-9A)	Co-Mo/Al_2O_3 (Cyanamid HDS-16A)	Ni-W/Al_2O_3 (Nalco NT-550)
k_1	5.0	3.1	7.7
k_2	36.2	19.0	43.0
k_3	7.2	3.67	4.0
k_5	0.38	0.015	0.15
k_4	8.8	2.91	3.77
k_6	1.14	0.43	0.41
k_8	2.20	0.79	0.77
k_7	2.19	0.73	0.76
$k_{total\ N\text{-}removal}$	1.25	0.48	0.54

Operating conditions: T = 367°C; P = 136 atm; All catalysts presulfided at 425°C for 2 hr in 10% H_2S in H_2; 0.05 wt % of CS_2 in white oil was used in all runs.

[Ni-Mo/γ-Al_2O_3] / [Co-Mo/γ-Al_2O_3]

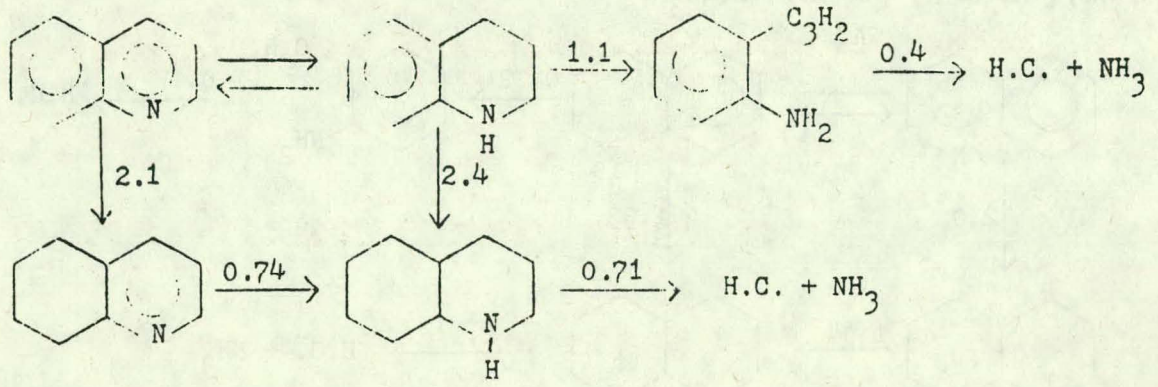

[Ni-W/γ-Al_2O_3] / [Co-Mo/γ-Al_2O_3]

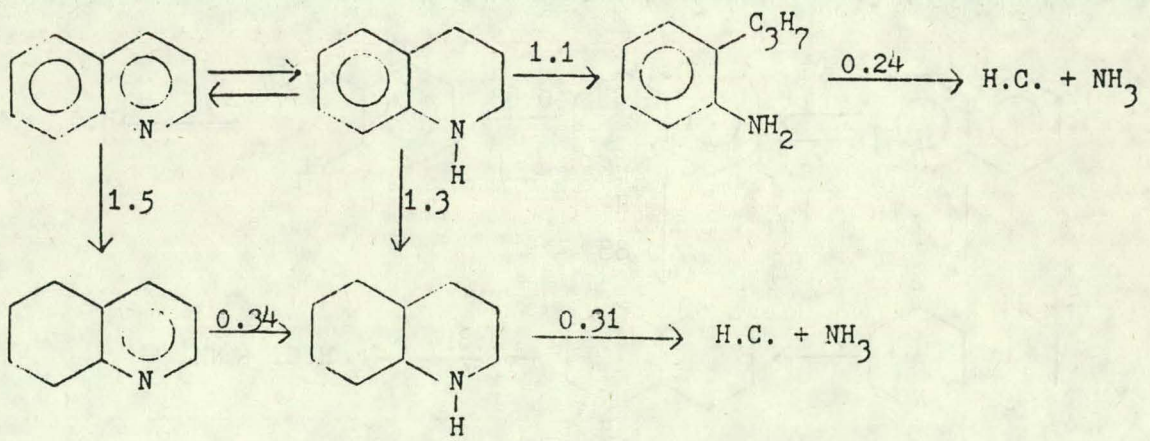

Figure B1. Relative kinetic behavior for quinoline hydrodenitrogenation normalized to the least active catalyst: standard conditions of Table I, no CS_2 added.

[Ni-Mo/γ-Al_2O_3] / [Co-Mo/γ-Al_2O_3]

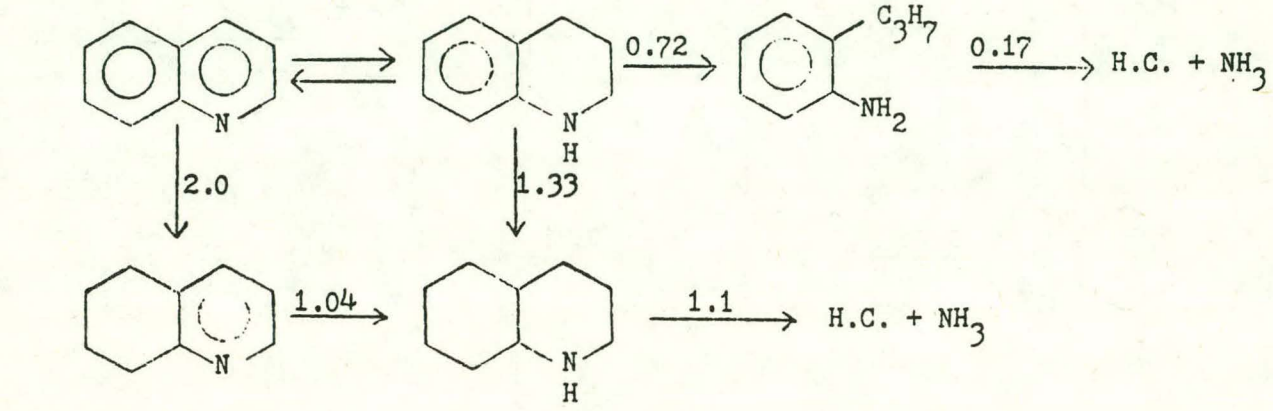

[Ni-W/γ-Al_2O_3] / [Co-Mo/γ-Al_2O_3]

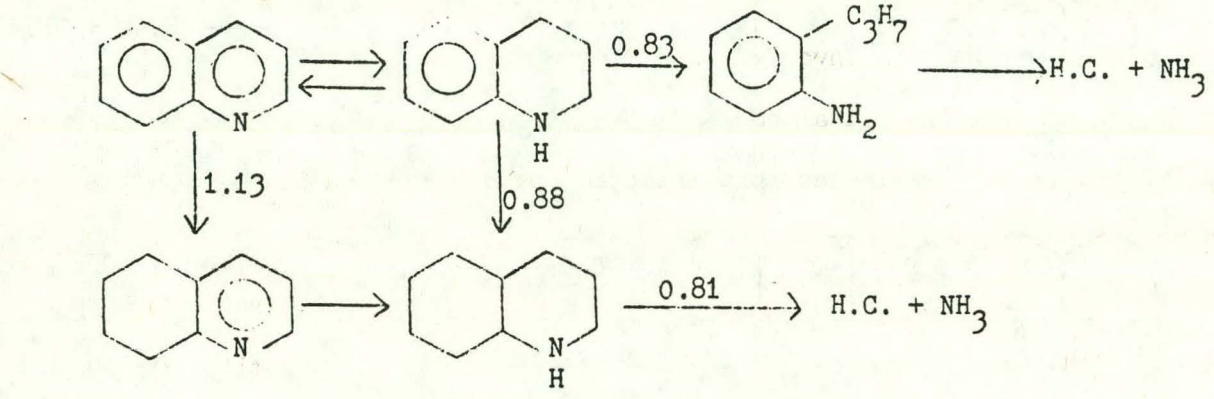

Figure B2. Relative kinetic behavior for quinoline hydrodenitrogenation normalized to the least active catalyst: standard conditions of Table I, with H_2S present in the gas phase (0.05 wt % CS_2 added).

H_2S present in the gas phase (CS_2 added).

The total nitrogen removal rates indicate that Ni-Mo/γ-Al_2O_3 is a somewhat better catalyst in the absence of H_2S and significantly better in the presence of H_2S (Tables III and IV) even though the relative rates of the essential cracking steps are less to only slightly higher for the Ni-Mo/γ-Al_2O_3. This occurs because the Ni-containing catalysts accelerate the rate of benzenoid ring hydrogenation leading to decahydroquinoline so that although the pseudo first-order rate constants for decahydroquinoline cracking are less, the rate of decahydroquinoline cracking and thus the total rate of nitrogen removal is greater because of the higher concentration of decahydroquinoline. For Co-Mo/γ-Al_2O_3, the formation of o-propylaniline is competing significantly with the formation of decahydroquinoline, the relative rate of formation of decahydroquinoline being only three times that of o-propylaniline; whereas for the Ni-Mo/γ-Al_2O_3, the relative rate is eight times. For Co-Mo/γ-Al_2O_3 both the reaction path involving o-propylaniline and that involving decahydroquinoline contribute significantly to nitrogen removal although the reaction path involving decahydroquinoline is clearly the more important path. For the Ni-Mo/γ-Al_2O_3 the reaction path involving decahydroquinoline clearly predominates. These same comments apply to Ni-Mo/γ-Al_2O_3. The substitution of W for Mo in the catalyst has the effect of slowing the rates of almost all reaction steps considerably. Also apparent is the fact that the rate determining step seems to be the hydrogenation of the aromatic and heteroaromatic rings. Even though k_1 is comparable to k_6 in value, the other pseudo first-order rate constants, which are smaller, and the equilibrium between quinoline and

1,2,3,4-tetrahydroquinoline, which strongly favors 1,2,3,4-tetrahydroquinoline, prevents rapid rates of total nitrogen removal.

Presulfiding a catalyst has a marked effect on the rate relationships within the quinoline network; the rate of total nitrogen removal doubles (Table II). Similar effects are seen in the individual reactions in the network. This is in accordance with earlier reports (Goudriaan, 1974; Voorhoeve, 1971; Voorhoeve and Stuiver, 1971) of the enhancement in hydrodenitrogenation catalyst activity upon presulfiding. However, this rate acceleration effect occurs only in the hydrogenation reactions; the carbon-nitrogen bond breaking steps are not increased significantly. There is even a small negative effect of presulfiding on the rate of these steps. Since hydrogenation activity is increased, the intermediate both partially and fully hydrogenated are formed more rapidly along the time axis for the presulfided catalyst leading to a more rapid nitrogen removal although the carbon-nitrogen bond breaking steps are not enhanced. The hydrogenation reactions involving the benzoid ring experienced up to a four-fold enhancement. This probably resulted because the metal sulfides formed upon sulfiding are more active for hydrogenation than the oxide form due to the structural and surface defect properties of the sulfided form (Schuit and Gates, 1973; Voorhoeve, 1971; Voorhoeve and Stuiver, 1971).

The presence of gas-phase H_2S causes a significant increase in the rate of hydrogenation of the heteroaromatic ring (Table V); we speculate that this may be due to an increase in the acidity of the surface induced by H_2S thus facilitating the interaction of the basic nitrogen atom of the heterocyclic ring with the catalyst surface. Conversely hydrogenation of the benzenoid ring is decreased by H_2S (K_1 and k_3 of Table III). This effect

is most apparent for the Ni-W/γ-Al_2O_3, which also shows the greatest increase in heteroaromatic ring hydrogenation. This is in accordance with Voorhoeve's (1971; Voorhoeve and Stuiver, 1971) results on the hydrogenation of benzene in the absence and presence of H_2S. These authors showed that CS_2 decreased the hydrogenation activity of NiS_2 and WS_2 and $NiWS_2$ catalysts. They also found that increasing H_2S concentration reduces the pre-experimental factor but not the activation energy, thus concluding that the active site is a sulfur deficient metal center. The Co-Mo/γ-Al_2O_3 catalyst was the least affected by the presence of H_2S in the system, whereas Ni-W/γ-Al_2O_3 was the most influenced. The reasons why the nickel-containing catalysts are more reactive in hydrogenation are not clear; but nickel-containing catalysts are typically better for aromatic hydrogenation (Ahuja et al., 1970).

For the carbon-nitrogen bond breaking steps, the effect of H_2S depends on the type of reaction and the type of catalyst. The largest effect on decahydroquinoline conversion to hydrocarbon and ammonia (k_6) occurs with the Ni-W/γ-Al_2O_3; for the Co-Mo/γ-Al_2O_3 the effect is almost negligible; and for Ni-Co/γ-Al_2O_3 shows intermediate behavior. For the Ni-containing catalysts H_2S may increase the surface acidity or draw Ni ions to the surface of the γ-Al_2O_3, whereas the Co-Mo/γ-Al_2O_3 catalyst may already present its optimum surface structure. Carbon-nitrogen bond breaking reactions involve essentially a secondary amine. In contrast, an aromatic amine (e.g., 1,2,3,4-tetrahydroquinoline) is less basic and H_2S causes an equal increase in k_4 for all three catalysts. Because of the less basic character for aromatic amines acidity of the surface by H_2S should assist adsorption and reaction. H_2S exerts a negative influence on the rate

of disappearance of o-propylaniline (k_5). Since H_2S has a negative influence on benzenoid ring hydrogenation, and since the major route for hydrodenitrogenation of this compound appears to involve first ring hydrogenation (Shih et al., 1977), the hydrogenation of the benzenoid ring should be impaired by H_2S.

The relative effect of increased operating severity on the hydrodenitrogenation of quinoline over Ni-Mo/γ-Al_2O_3 and Co-Mo/γ-Al_2O_3 is shown in Figure B3. Under these more severe conditions, Ni-Mo/γ-Al_2O_3 is substantially the better catalyst for each of the steps in the reaction network. Higher temperature favors cracking of the C-N bond in tetrahydroquinoline the relative disappearance of o-propylaniline is consistent with independently determined results involving this reagent with both catalysts. Again kinetically the most important reactions are the hydrogenation reactions. For the Co-Mo/γ-Al_2O_3 the increase in severity of the operating conditions results in a decrease in the rate of hydrogenation from quinoline to 5,6,7,8-tetrahydroquinoline. This may be an artifact of the measurement because under these conditions the quinoline concentration was very low or it may be due to the negative dependence of rate on dihydrogen pressure in this pressure range (Shih et al., 1977).

Acridine hydrodenitrogenation

As with quinoline hydrodenitrogenation under the more severe conditions, for acridine the catalyst activity clearly follows Ni-Mo/γ-Al_2O_3 > Ni-W/γ-Al_2O_3 > Co-Mo/γ-Al_2O_3. The acridine network shows parallel behavior in that the aromatic rings have to be hydrogenated before nitrogen removal can occur. Kinetically the hydrogenation reactions are clearly important although they have relatively less effect on the rate of total nitrogen than

$[Ni\text{-}Mo/\gamma\text{-}Al_2O_3]$ / $[Co\text{-}Mo/\gamma\text{-}Al_2O_3]$

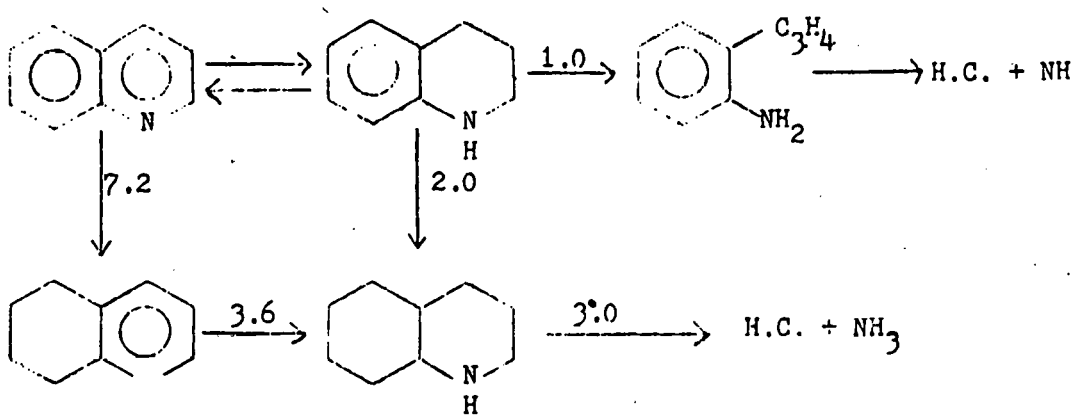

Figure B3. Relative kinetic behavior for quinoline hydrodenitrogenation at more severe conditions: 367°C, 136 atm presulfided catalysts with 0.05 wt % CS_2 added.

for quinoline. As shown in Table VII, k_1, k_2, k_3 and k_4 far outweigh the magnitude of the pseudo first-order rate constants for carbon-nitrogen bond breaking. Even though k_5 is smaller than any of the carbon-nitrogen bond-breaking reactions, the network contains an alternate predominant route to prehydroacridine.

The relative kinetic behavior of the three catalysts in acridine hydrodenitrogenation is shown in Figures B4 and B5. Replacing Co with Ni results in very substantial increases in the relative rates of each of the reactions in the acridine network. The Ni-W/γ-Al_2O_3 shows similarly enhanced activity over Co-Mo/γ-Al_2O_3. The higher activity is observed for both the hydrogenation reactions and for the carbon-nitrogen bond breaking reactions. The largest effect of Ni appears in the hydrogenation of the heteroaromatic ring in symoctahydroacridine. Hydrogenation of symoctahydroacridine is the slowest reaction in the acridine reaction network (Table VII) and thus this reaction becomes extremely important catalytically, and a catalyst which is relatively more active for catalyzing this reaction will probably also appear to be a better catalyst for total nitrogen removal.

The Ni-W/γ-Al_2O_3 is no more active for carbon-nitrogen bond rupture than Co-Mo/γ-Al_2O_3. Since this is kinetically an important step in acridine hydrodenitrogenation, the higher activities of the Ni-W/γ-Al_2O_3 for the hydrogenation reactions does not effectively result in substantially higher activity for total nitrogen removal (Table VII). Figure B5 also demonstrates this point. The rates of the early hydrogenation reactions are higher on Ni-W/γ-Al_2O_3 but for all of the later hydrogenation reactions and the carbon-nitrogen bond breaking reactions the Ni-Mo/γ-Al_2O_3 is about 2.5 times

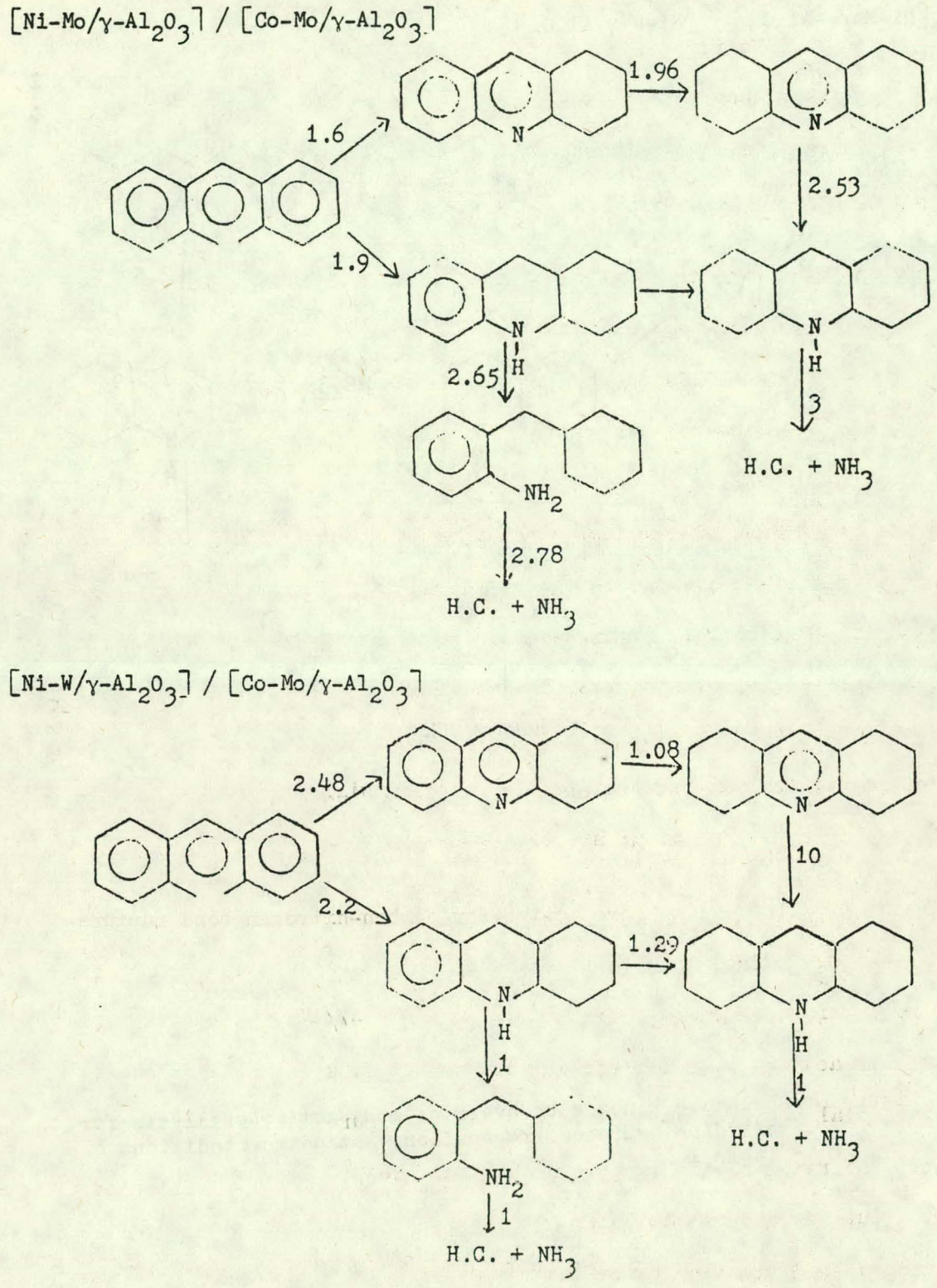

Figure B4. Relative kinetic behavior for acridine hydrodenitrogenation normalized to the least active catalyst: standard conditions of Table I. 367°C, 136 atm, 1.4 vol % H_2S in the gas phase.

$[Ni\text{-}Mo/\gamma\text{-}Al_2O_3] / [Ni\text{-}W/\gamma\text{-}Al_2O_3]$

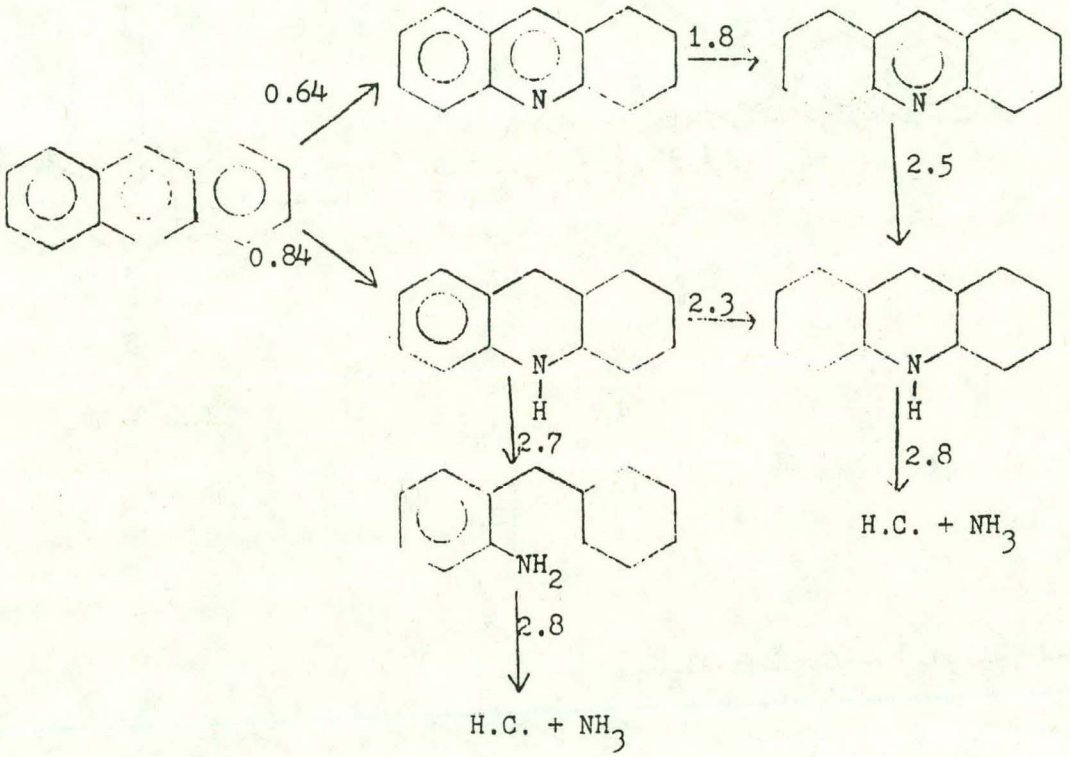

Figure B5. Relative kinetic behavior of most active catalysts for acridine hydrodenitrogenation: standard conditions of Table I.

more active. Chemical and mechanistic explanations for these differences require further study.

Conclusions

Because of the complexity of the hydrodenitrogenation reaction network, involving hydrogenation and carbon-nitrogen bond rupture as distinct reactions, the evaluation and further development of HDN catalysts can be greatly aided by knowledge of the rate of the various intermediate reaction steps in the reaction network. This work shows that Ni-Mo/Al_2O_3 is typically better for hydrodenitrogenation because it has higher hydrogenation activity than Co-Mo/Al_2O_3; Ni-W/Al_2O_3 appears to be slightly less active than Ni-Mo/Al_2O_3. The cracking activities appear to be more dependent on the source of the support and are also important in determining the relative ranking of overall catalyst behavior. This aspect of catalyst behavior was not sufficiently investigated in this work to allow for firm conclusions.

This also shows that complex reaction networks can effectively be analyzed and that information gained in this analysis can be used and interpreted in a way that should foster and promote the rational design and development of new and improved catalysts.

LITERATURE CITED

Aboul-Gheit, A. K., and Abdou, I. K., J. Institute of Petroleum 59, 188 (1973).

Aboul-Gheit, A. K., Can J. Chem. 53, 2575 (1975).

Ahuja, S. P., Derrien, M. L., and Le Page, J. E., Ind. Eng. Chem. Prod. Res. Develop. 9, 272 (1970).

Cir, J., and Kubicka, R., Erdol Konle Erdgas Petrochem 25, (4), 181 (1972).

Doelman, J., and Vlugter, J. D., Proc. Sixth World Petroleum Congr. Section III, p. 247, The Hague, The Netherlands, 1963.

Flinn, R. A., Larson, O. A., and Beuther, H., Hydrocarbon Processing and Petrol. Refiner 42, No. 9, 129 (Sept., 1963).

Houalla, M., Broderick, D., de Beer, V. H. J., Gates, B. C., and Kwart, H., Division of Petroleum Chemistry Preprints, Vol. 22, No. 3, p. 941 (1977).

McIlvried, H. G., Ind. Eng. Chem., Process Des. Develop. 10, 125 (1971).

Rollmann, L. D., J. Catal. 46, 243 (1977).

Satterfield, C. N., and Coccetto, J. F., Ind. Eng. Chem., Process Des. Dev., 15, 272 (1976).

Schuit, G. C. A., and Gates, B. C., A.I.Ch.E. Journal 19, 417 (1973).

Shih, S. S., Katzer, J. R., Kwart, H., and Stiles, A. B., "Quinoline Hydrodenitrogenation: Reaction Network and Kinetics," submitted to J. Catal., 1977.

Shih, S. S., Katzer, J. R., Kwart, H., and Stiles, A. B., Division of Petroleum Chemistry Preprints, Vol. 22, No. 3, p. 919 (1977a).

Silver, H. F., Wang, N. H., Jensen, H. B., and Poulson, R. E., Amer. Chem. Soc., Preprints Div. Petrol Chem. 17, (4), G94 (1972).

Silver, H. F., Wang, N. H., Jensen, H. B., and Poulson, R. E., "A Comparison of Shale Gas Oil Denitrification Reactions over Co-Mo and Ni-W Catalysts," Paper at Amer. Chem. Soc. Meeting, Los Angeles, March, 1974.

Sonnemans, J., Neyens, W. J., and Mars, P., J. Catal. 34, 215 (1974), 34, 230 (1974).

Sonnemans, J., and Mars, P., J. Catal. 31, 209 (1973).

Sonnemans, J., Van Den Berg, G. H., and Mars, P., J. Catal. 31, 220 (1973a).

Sonnemans, J., Goudriaan, F., and Mars, P., in Catalysis, Proceedings of the Fifth International Congress on Catalysis," ed. J. W. Hightower, p. 76-1085, North-Holland Pub. Co., Amsterdam, 1973b.

Voorhoeve, R. J. H., J. Catal. 23, 236 (1971).

Voorhoeve, R. J. H., and Stuiver, J. C. M., J. Catal. 23, 228; 243 (1971).

Yarrington, R. M., Paper presented at 19th Canadian Chemical Engineering Conference and Third Symposium on Catalysis, Edmonton, 1969.

Zawadzki, R., Shih, S. S., Katzer, J. R., and Kwart, H., "Kinetics of Acridine Hydrodenitrogenation," submitted to J. Catal.

C. POISONING REACTION ENGINEERING

In the previous quarterly reports, both the physical and chemical properties of the aged catalyst used in coal-derived liquid hydroprocessing were examined. The catalyst samples are from the Synthoil process, H-Coal^R process and a proprietary process. It was concluded that both mineral matter deposits and coke contribute primarily to the deactivation of the catalyst. The result of regeneration of H-Coal^R catalyst of Run No. 130-78 (1502 lb coal/lb catalyst) showed that the coke accumulation was up to approximately 22 wt % and the analysis by mercury penetration of the pore volume for a catalyst sample from the Synthoil process showed that 50% to 70% of the pore volume has been lost during the hydroprocessing. These experimental observations imply that coking may not only reduce the catalyst activity by occupying the active sites but also change the macrostructures of the catalyst such as pore volume and effective pore size, which will have substantial effects on the transport properties. The pore plugging effect will become more serious especially in the hydrotreating process containing large species such as asphaltenes. Since most of the area of the catalyst was in the micropores within the range of 10-100 Å for all the catalyst samples examined, and the diameters of asphaltenes are reported to lie in the range of 15-60 Å, strong configurational exclusion effects in combination with the pore plugging would be expected. These effects will diminish the catalyst life by both the deactivation of active site and the blockage of pore mouths to inhibit the access of reactant molecules through the narrowed pores.

In this report, an attempt to study the coke deposition on the catalyst behavior in H-Coal^R process is described. The essence of this

theoretical investigation is to obtain the qualitative informations for reactor design and selection of catalysts for long catalyst life.

In order to demonstrate the simultaneous effect of geometrical exclusion and pore plugging due to the coke deposition in the ebullated bed H-Coal^{R} process, a typical mechanism of impurity fouling is considered as follows:

$$c \xrightarrow{K_1} b \text{ (main reaction)}$$

$$p \longrightarrow \bar{p} \text{ (coking)}$$

Where c is the reactant, b is the desired product, p is the coke precursor and $\bar{p}$ is the coke deposit on the catalyst surface.

Assuming that the total amount of hydrogen dissolved in the liquid phase under high pressure-operating conditions is sufficient for the consumption needed, the mass-transfer limitation in the liquid phase will be predominant. The constitutive equations characterize the system of an isothermal, continuous stirred tank reactor are:

Material balance for fluid phase:

$$v_o c_o - v_o c - K_{f,1} S^* V^* (c - c_o) = 0 \qquad (1)$$

$$v_o p_o - v_o p - K_{f,2} {}^* S^* V^* (p - p_o) = 0 \qquad (2)$$

Where, c_o = concentration of reactant in feed stream

p_o = concentration of coke precursor in feed stream

v_o = volumetric flow rate of feed stream

V = total volume of the reactor

$K_{f,1}; K_{f,2}$ = mass transfer coefficients in liquid phase(cm/sec)

S = external surface area of catalyst per unit volume of reactor

Material balance for single pellet :

$$\frac{1}{r^2}\frac{\partial}{\partial r}\left(r^2 D_{e,1}\frac{\partial \tilde{C}}{\partial r}\right) = K_1 \theta^{\alpha} \tilde{C}^{\beta} \tilde{P}^{\gamma} \rho_c \qquad (3)$$

$$\frac{1}{r^2}\frac{\partial}{\partial r}\left(r^2 D_{e,2}\frac{\partial \tilde{P}}{\partial r}\right) = K_2 \theta^{\delta} \tilde{P}^{\gamma} \rho_c \qquad (4)$$

$$\frac{\partial \bar{P}}{\partial t} = -K_2 \theta^{\delta} \tilde{P}^{\gamma} \qquad (5)$$

with the following boundary conditions :

$$\left.\frac{\partial \tilde{C}}{\partial r}\right|_{r=0} = 0$$

$$\left.\frac{\partial \tilde{P}}{\partial r}\right|_{r=0} = 0$$

$$D_{e,1}\left.\frac{\partial \tilde{C}}{\partial r}\right|_{r=r_p} = k_{f,1}\left(C - \tilde{C}|_{r=r_p}\right)$$

$$D_{e,2}\left.\frac{\partial \tilde{P}}{\partial r}\right|_{r=r_p} = k_{f,2}\left(P - \tilde{P}|_{r=r_p}\right) \qquad (6)$$

Where, $D_{e,i}$ = effective diffusivity for ith component.

θ = catalyst activity.

$\alpha, \beta, \gamma, \delta$ = exponents of reaction order.

ρ_c = density of catalyst pellet

The fractional activity, θ, of the catalyst is defined to be

$$\theta = 1 - \bar{P}/P_s \qquad (7)$$

Here $\bar{p}_s$ specifies the saturated coke deposition on catalyst surface.

Consider the typical cylindrical pore structure with initial pore radius R_o and assume the coke deposition is monotonous as shown in Fig. C1. Then the effective pore size as a function of catalyst activity can be described as

$$\left(\frac{\tilde{r}}{R_o}\right)^2 = 1 - (1-\theta)/NPU \qquad (8)$$

Where NPU characterizes the number of poison unit and is defined as follows

$$NPU = \bar{p}_{max}/\bar{p}_s \qquad (9)$$

Here $\bar{p}_{max}$ specifies the maximum amount of coke concentration as the pores are filled with coke completely.

On consideration of geometrical exclusion effect of the diffusion process of large molecule through a fine pore, the emperical correlation proposed by Satterfield et al. (1973) can be applied

$$D_{e,i} = \frac{D_{o,i}\,\epsilon}{\tau}\, e^{-4.6\lambda_i} \qquad (10)$$

Where ϵ = fractional free cross section area.

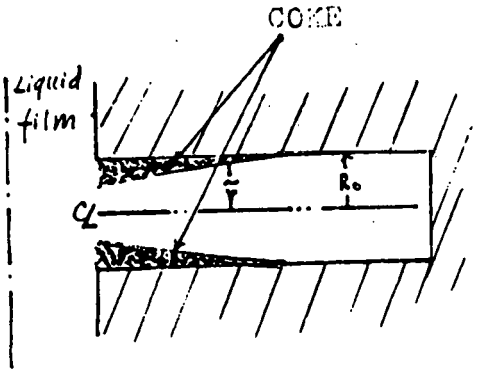

Figure C1. Deposition of coke in a cylindrical catalyst pore.

τ = tortuosity factor.

λ_i = geometrical ratio of reactant molecule with respect to pore size for ith component

We define the correction factor of effective diffusivity to be the ratio of the effective diffusivity in the pore-plugged catalyst to that in the fresh catalyst, and we get

$$\alpha_{d,i} = \left[1 - \frac{(1+\theta)}{N\pi}\right] \exp\left\{\frac{-4.6\,\lambda_{o,i}}{\sqrt{1-\frac{(1+\theta)}{N\pi}}}\right\} \qquad (11)$$

where λ_o specifies the geometrical ratio in fresh catalyst.

Defining the dimensional and the dimensionless groups as follows :

$$\tilde{C} = \frac{\tilde{C}}{C_o} \; ; \; \tilde{P} = \frac{\tilde{P}}{P_o} \; ; \; \phi = \frac{c}{C_o} \; ; \; P = \frac{P}{P_o}$$

$$f = \frac{V}{V_p}$$

$$LHSV = \frac{V_o}{V}$$

$$\tau_{p,i} = \frac{V_p^2}{De,i} \quad (\text{diffusion time})$$

$$Bo,i = \frac{K f_{2i} \cdot V_p}{De,i}$$

$$\phi_c = V_p \sqrt{\frac{K_1 C_o^{\beta-1} \rho_c}{De,1}}$$

$$\phi_p = V_p \sqrt{\frac{K_2 P_o^{\gamma-1} \rho_c}{De,2}}$$

$$\tau = (t \cdot K_2 P_o^{\gamma}) / \bar{P}_s$$

V_c = fractional volume of catalyst

then the original equations characterizing the catalyst behavior in H-Coal^R Hydroprocessing can be rearranged to be :

Fluid phase

$$= \frac{\frac{1}{Bo,1} + \frac{3\,V_c}{LHSV \cdot \tau_{p,1}} \tilde{\phi}\Big|_{\rho=1}}{\frac{1}{Bo,1} + \frac{3\,V_c}{LHSV \cdot \tau_{p,1}}} \qquad (12)$$

$$1 = \frac{\frac{1}{Bo,2} + \frac{3V_c}{\angle HSV \cdot \tau_{p,2}} \tilde{P}\big|_{\rho=1}}{\frac{1}{Bo,2} + \frac{3V_c}{\angle HSV \cdot \tau_{p,2}}} \tag{13}$$

Catalyst pellet

$$C_{d,1} \nabla^2 \tilde{C} + \frac{\partial C_{d,1}}{\partial \rho} \frac{\partial \tilde{C}}{\partial \rho} = \phi_c^2 \theta^{\alpha} \tilde{C}^{\beta} \tag{14}$$

$$C_{d,2} \nabla^2 \tilde{P} + \frac{\partial C_{d,2}}{\partial \rho} \frac{\partial \tilde{P}}{\partial \rho} = \phi_p^2 \theta^{\delta} \tilde{P}^{\gamma} \tag{15}$$

$$\frac{\partial \theta}{\partial \tau} = -\theta^{\delta} \tilde{P}^{\gamma} \tag{16}$$

And the boundary conditions become :

$$\frac{\partial \tilde{C}}{\partial \rho}\Big|_{\rho=0} = 0$$

$$\frac{\partial \tilde{P}}{\partial \rho}\Big|_{\rho=0} = 0$$

$$C_{d,1} \frac{\partial \tilde{C}}{\partial \rho}\Big|_{\rho=1} = \left[\frac{1}{\frac{1}{Bo,1} + \frac{3V_c}{\angle HSV \cdot \tau_{p,1}}}\right] (1 - \tilde{C}|_{\rho=1}) \tag{17}$$

$$C_{d,2} \frac{\partial \tilde{P}}{\partial \rho}\Big|_{\rho=1} = \left[\frac{1}{\frac{1}{Bo,2} + \frac{3V_c}{\angle HSV \cdot \tau_{p,2}}}\right] (1 - \tilde{P}|_{\rho=1})$$

$$\theta(\rho, \tau=0) = 1.$$

The effect of coke deposition on the main reaction can be characterized by the effectiveness factor defined as the ratio of the observed reaction rate to the initial rate in the absence of mass transfer resistance, i.e.,

$$\eta(\tau) = \frac{\int_0^1 \phi_c^2 \theta^{\alpha} \tilde{C}^{\beta} \rho^2 d\rho}{\int_0^1 \phi_c^2 \theta^{\alpha} \tilde{C}^{\beta} \rho^2 d\rho\big|_{\tau=0,\rho=1}} \tag{18}$$

The total activity is simply related to the fraction of the initial effectiveness factor which remains after the coking has started. This fractional activity ratio is then defined to be :

$$A(\tau) = \frac{\eta(\tau)}{\eta(0)} \qquad (19)$$

The prediciton o. the amount of coke laydown per unit volume of reactor can be derived to be :

$$W(\tau) = (360 \rho_p V_c) \int_0^1 \frac{(t-\theta)}{N p a} \rho^2 d\rho \qquad (20)$$

And the deviation of the effective diffusivity by coke laydown can be characterized by the average correction factor as follows

$$\widetilde{C_d} = 3 \int_0^1 C_{d,i} \rho^2 d\rho \qquad (21)$$

For the sake of demonstration of the coke effect on the performance of the H-Coal^R reactor, a reaction network with $\alpha = \beta = \gamma = \gamma = 1$ is considered. Some secondary parameters are assumed as follows:

$$E_{o,i} = 1000 \quad ; i=1,2$$
$$LHSV = 1 \text{ hr}^{-1}$$
$$V_c = 0.5$$
$$\tau_{p,i} = 1 \text{ hr} \quad ; i=1,2$$

The numerical results are shown in Figs. C2 to C7. Some quali-

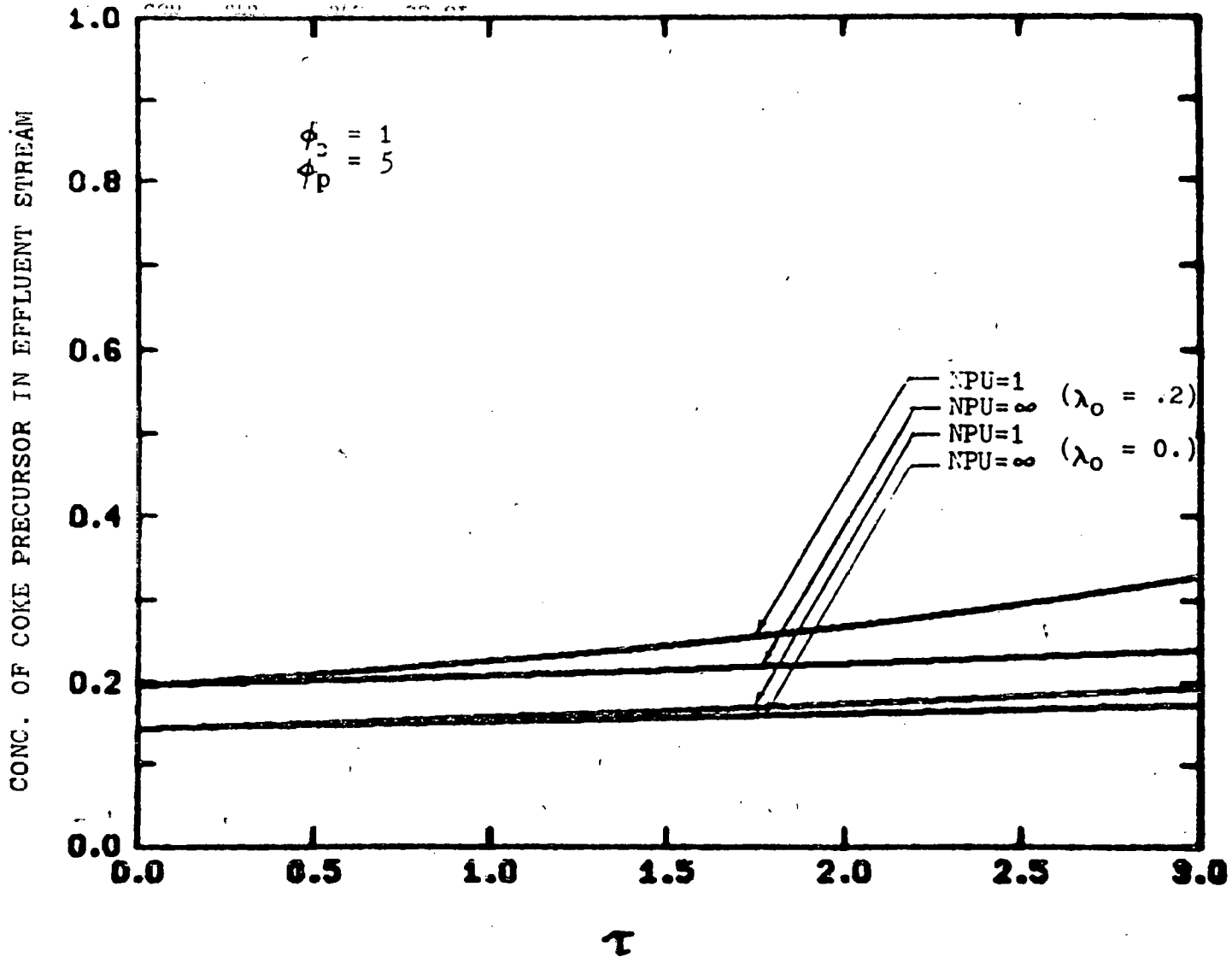

Figure C2. The geometrical exclusion and pore plugging effects on the time change of the concentration of coke precursor in effluent stream.

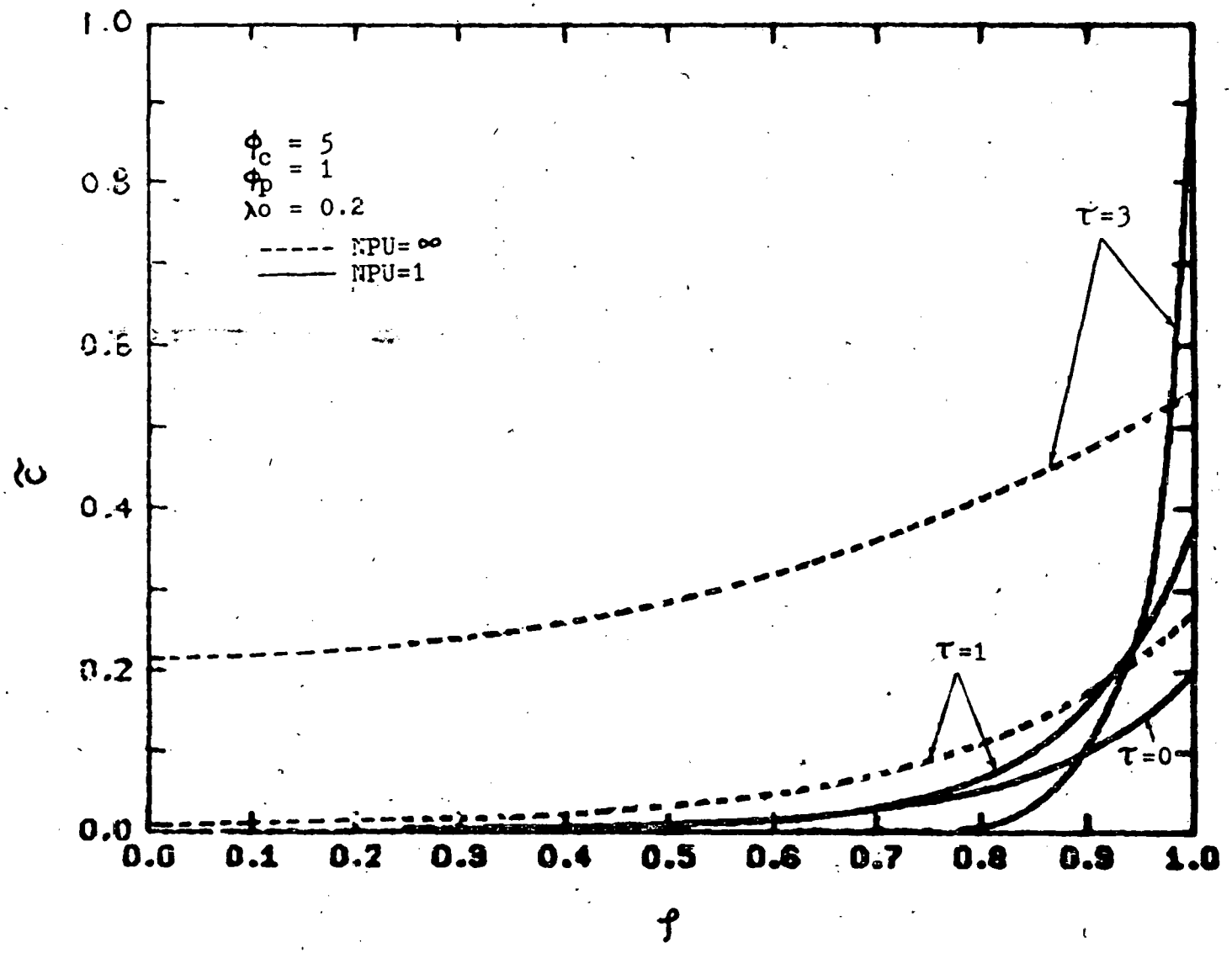

Figure C3. Concentration profiles of main reactant inside a catalyst pellet.

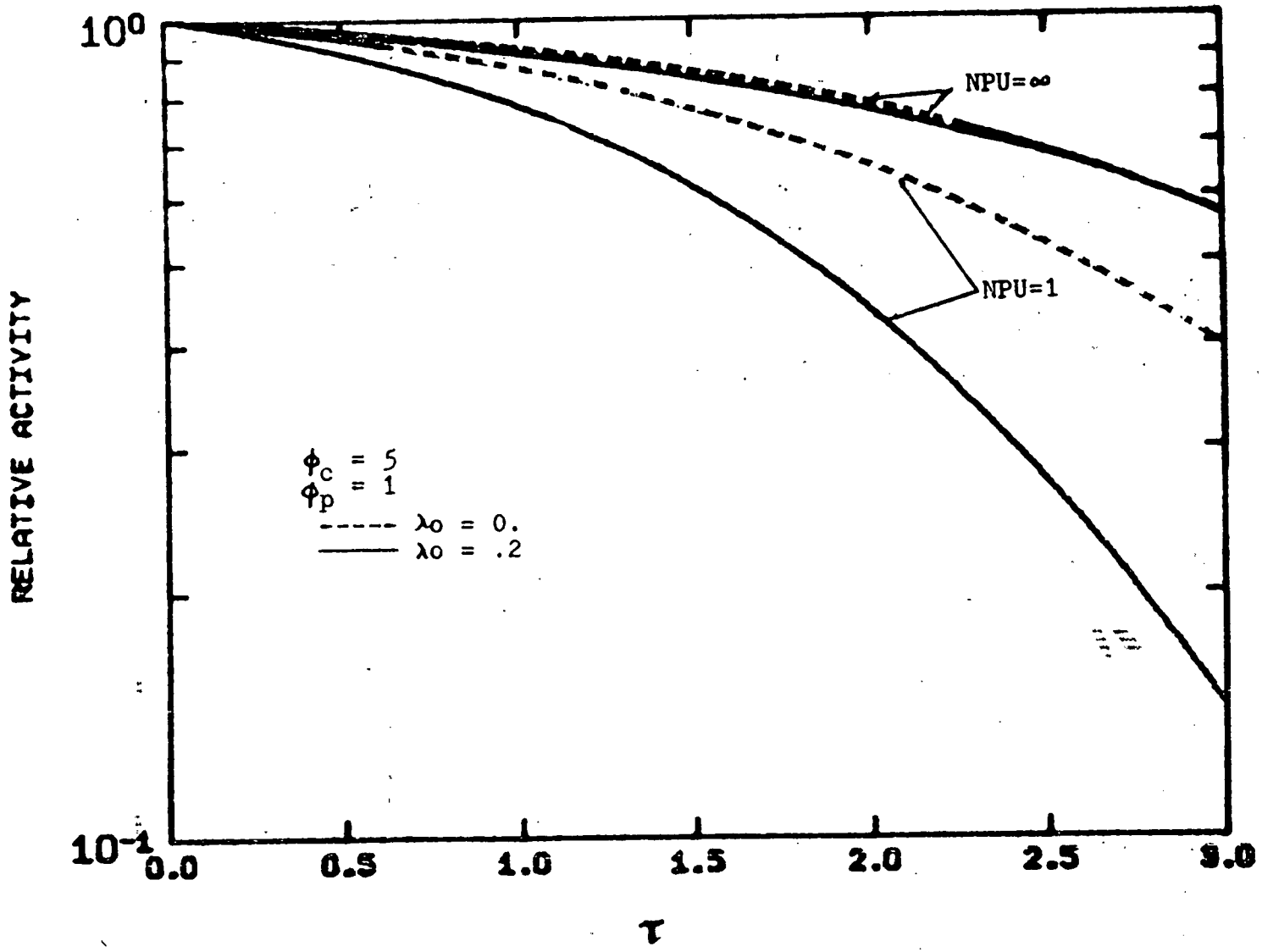

Figure C4. Dependence of relative activity on the effects of pore plugging and configurational diffusion limitation.

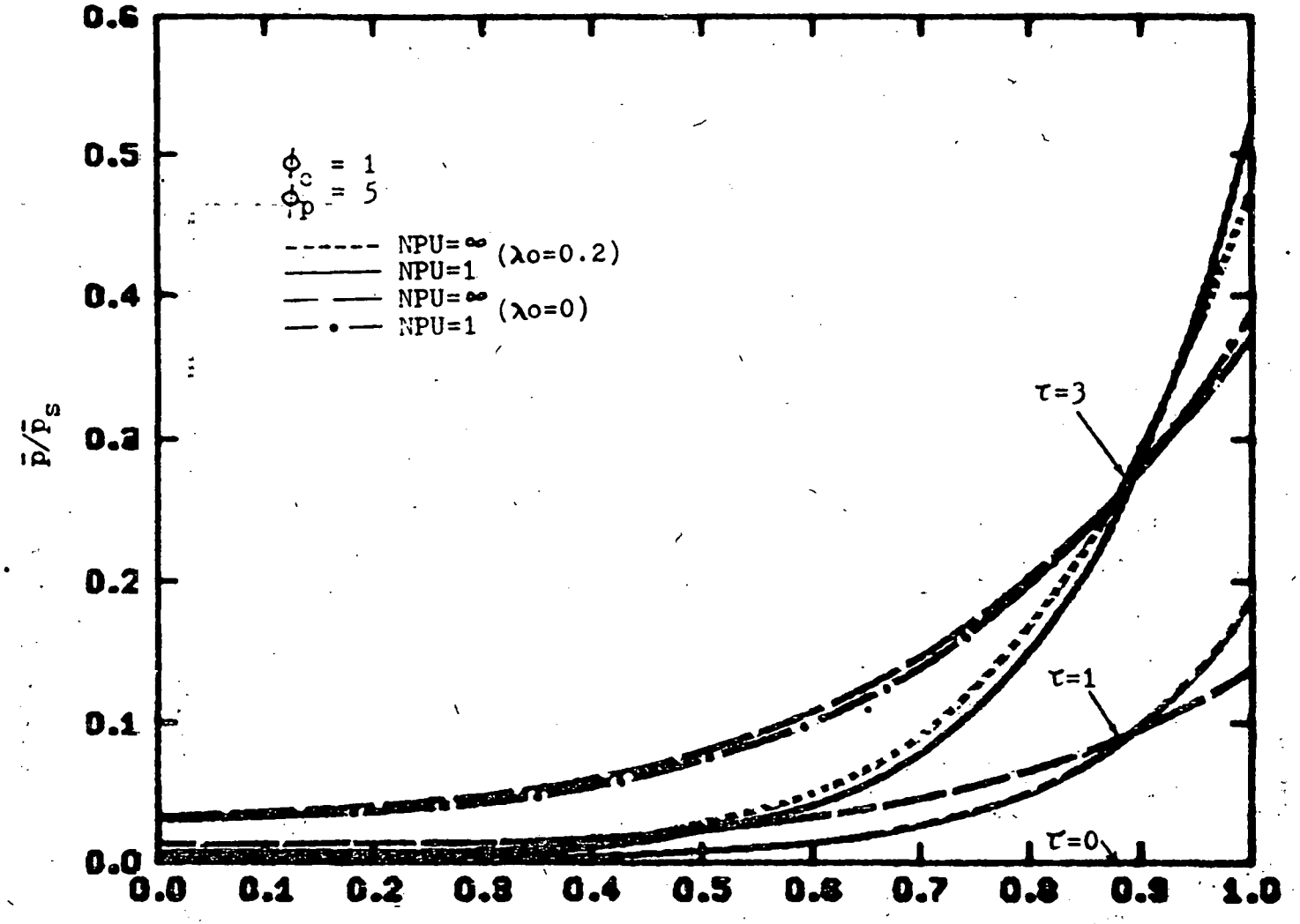

Figure C5. Time change of coke profile inside a catalyst pellet.

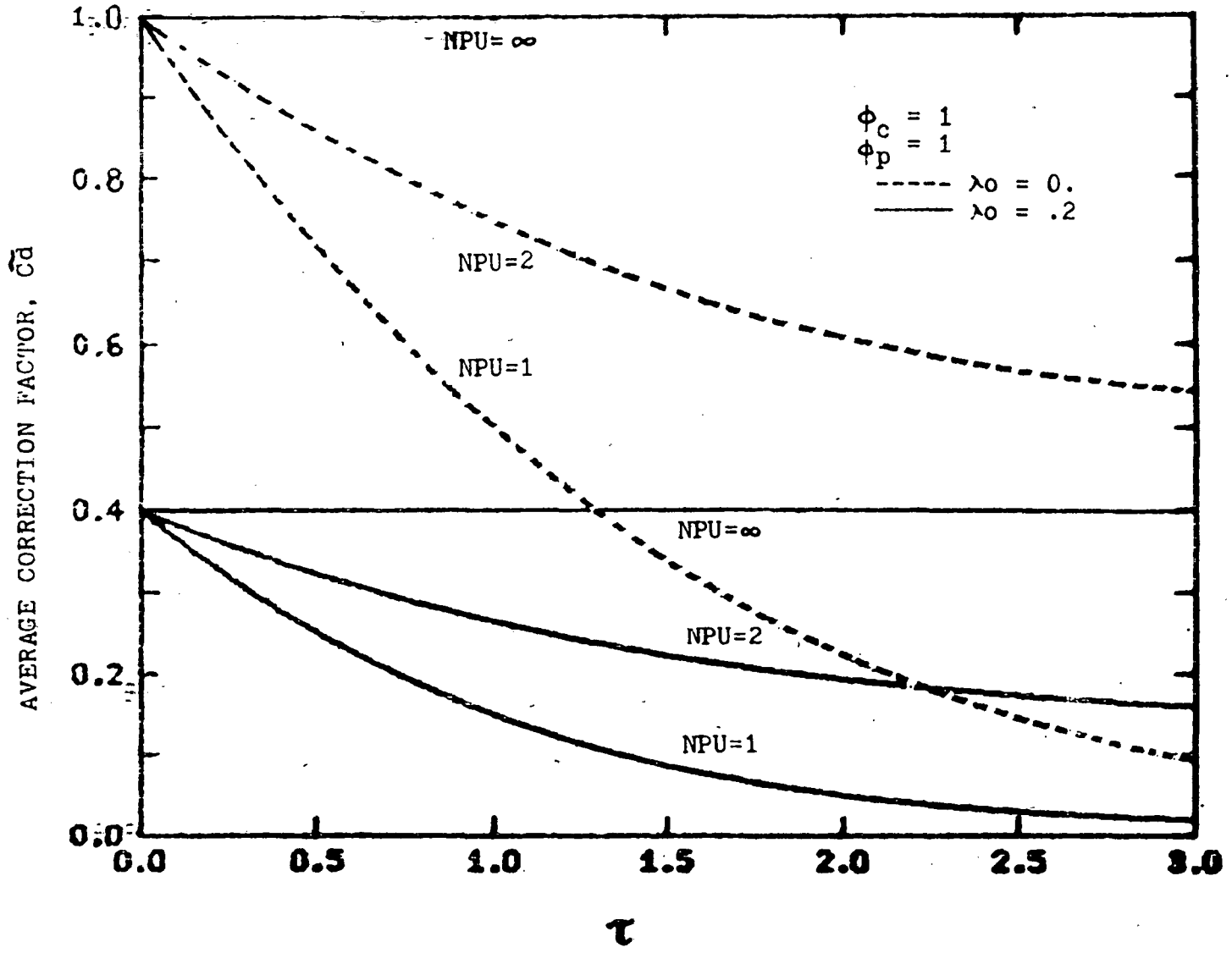

Figure C6. Decrease of effective diffusivity, apparent in consideration of both pore plugging and geometrical exclusion effects.

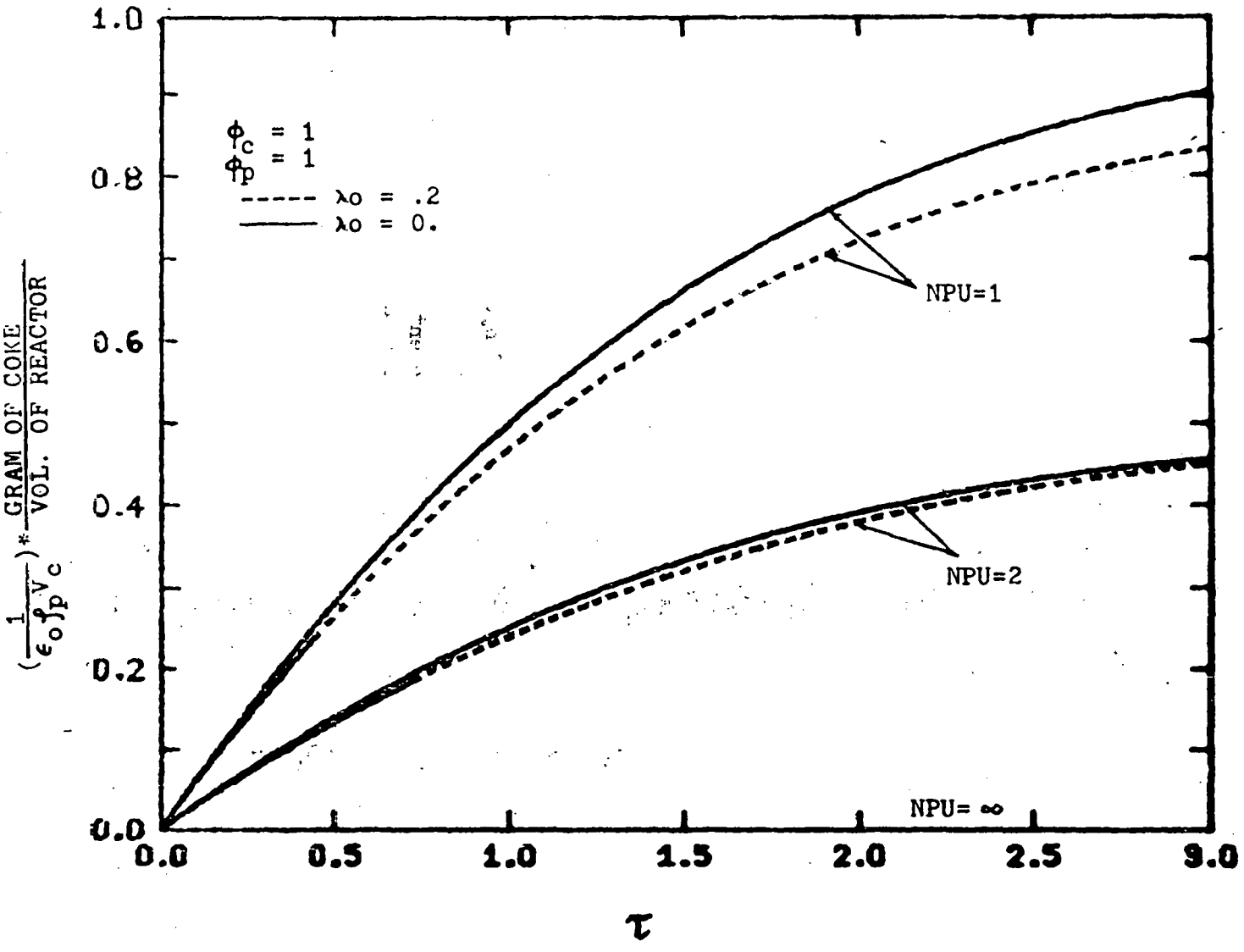

Figure C7. Prediction of total coke laydown per unit volume of reactor bed.

tative remarks will be discussed below.

Fig. C2 shows the time change of the concentration of coke precursor in the effluent stream for a typical Thiele moduli of $\phi_c = 1$ and $\phi_p = 5$. From this figure it is found when λ_o is increased, i.e., the geometrical exclusion effect becomes significant, the degree of coke formation will be lessened. Therefore, the concentration of coke precursor in the effluent stream will increase. And a pore plugging effect appears significant in consideration of a configuration diffusion limitation. It implies that the optimum selection of catalyst pore size will be effective to avoid coke formation. The examination of the concentration profile of main reactant inside the catalyst pellet is shown in Fig. C3. The effect of coke deposition on the concentration profile is obvious for the typical case of $\lambda_o = 0.2$. While the reactant penetrates deeply into the interior of catalyst pellet for NPU = ∞, there appears a sharp gradient for NPU = 1. The prevention of the access to the interior of the catalyst due to the pore plugging will eliminate the penetration depth of reactant molecules.

The efficiency of catalytic reaction can be specified in terms of relative activity as shown in Fig. C4. Without consideration of configurational diffusion limitations, i.e., $\lambda_o = 0$., the discrepancy of relative activity between NPU = 1 and ∞ depends strongly on the coke deposit. The coupling effects of geometrical exclusion and pore plugging will further decrease the relative activity significantly. This is due to the substantial elimination of the large molecules passing through the narrowed pores. In contrast to coke formation, larger pore size will be favorable for higher

relative activity. Fig C5 shows the typical coke deposition profile in the catalyst pellet for higher Thiele modulus of coking reaction, i.e., ϕ_p=5. As the independent fouling mechanism is concerned, the coke deposit will accumulate preferentially in a peripheral shell and move toward the center. The configurational diffusion limitation will account for the sharp gradient of the coke profile along the pellet. Negligible amounts of coke will be detected in the core of the catalyst when the geometrical factor, λ_o, is increased sufficiently.

The significant decrease in effective diffusivity due to the alternative effects of pore plugging and configurational exclusion is shown in Fig. C6. In the case of λ_o = 0, i.e., without configurational limitation, the result shows the mass flux through the diffusional process may be hindered severely due to coke deposits. The case of λ_o = 0.2 specifies that a further limitation of mass flux through the narrowed pore will occur due to the geometrical exclusion effect. The significant decrease of effective diffusivity will account for the shorter penetration depth and the low relative activity, as shown in previous figures.

In Fig. C7, the total coke laydown per unit volume of reactor is predicted. As expected, it shows that the coke laydown will be inversely proportional to the geometrical exclusion factor, λ_o, and the coke laydown appears to depend strongly on the number of NPU which characterizes the properties of both catalyst and fouling precursor.

In summary, in the above discussion catalyst deactivation due to coke laydown has been considered. A kinetic model of pore plugging and

geometrical exclusion effects is proposed to account for the high content of coke and the reduction of pore volume observed in the spent catalysts we have examined. The results suggest that catalysts with small pore size will be favorable to eliminate coke formation on the catalyst surface for the independent fouling mechanism in the H-Coal^{R} process. A further study based on quantitative information would be necessary to carry the evaluation further.

Reference for Part C

Satterfield C. N., Colton, C. K. and Pitcher, W. H., Jr. AIChE J. 19, 628 (1973).

V. CONCLUSIONS

HDS catalysts have been observed to undergo changes in activity during operation which are attributed to structural changes varying the number of catalytic sites; apparently some catalysts become sulfur deficient in the absence of enough H_2S. Reactor startup therefore requires sufficient H_2S in contact with the catalyst at all times.

Evaluation of HDN catalysts can be greatly aided by knowledge of reaction networks. The Ni-Mo/Al_2O_3 catalyst is better for HDN than Co-Mo/Al_2O_3 since it has higher hydrogenation activity. Hydrogenolysis (cracking) activity depends on the support and is also of importance in determining overall HDN activity, since the hydrogenation and cracking reactions in typical networks (quinoline, acridine) proceed at roughly equal rates.

A reaction engineering analysis of catalyst aging in the H-Coal^R process is outlined. Its proper evaluation awaits data from the H-Coal^R process.

VI. PUBLICATIONS

1. Stanulonis, J. J., B. C. Gates, and J. H. Olson, "Catalyst Aging in a Process for Liquefaction and Hydrodesulfurization of coal," A.I.Ch.E. Journal 19, 417 (1976).

2. Eliezer, Kenneth F., Manoj Bhinde, Marwan Houalla, Dennis Broderick, Bruce C. Gates, James R. Katzer, and Jon H. Olson, "A Flow Microreactor for Study of High-Pressure Catalytic Hydroprocessing Reactions," Ind. Eng. Chem. Fundamentals, 16, 380 (1977).

3. Chiou, M. J., and J. H. Olson, "A Method for Determining Catalytic Kinetics in a Pulse Microreactor System," submitted to Chem. Eng. Sci.

4. Houalla, M., D. Broderick, V.H.J. de Beer, B. C. Gates, and H. Kwart, Preprints, ACS Div. Petrol. Chem., 22 (3), 941 (1977).

5. Shih, S. S., J. R. Katzer, H. Kwart, and A. B. Stiles, Preprints, ACS Div. Petrol. Chem., 22 (3), 919 (1977).

VII. PERSONNEL

Dr. Marwan Houalla is leaving the group, and plans call for operating with a small group for several months to reduce expenditures. Several new workers may join in the fall.

*U.S. GOVERNMENT PRINTING OFFICE : 1979 0-620-097/2204